Noname manuscript No.
(will be inserted by the editor)

Reduced basis approximation and a posteriori error estimation for Stokes flows in parametrized geometries: roles of the inf-sup stability constants

Gianluigi Rozza · D.B. Phuong Huynh · Andrea Manzoni

the date of receipt and acceptance should be inserted later

Abstract

In this paper we review and we extend the reduced basis approximation and *a posteriori* error estimation for steady Stokes flows in affinely parametrized geometries, focusing on the role played by the Brezzi's and Babuška's stability constants. The crucial ingredients of the methodology are a Galerkin projection onto a low-dimensional space of basis functions properly selected, an affine parametric dependence enabling to perform competitive Offline-Online splitting in the computational procedure and a rigorous *a posteriori* error estimation on field variables. The combination of these three factors yields substantial computational savings which are at the basis of an efficient model order reduction, ideally suited for real-time simulation and many-query contexts (e.g. optimization, control or parameter identification). In particular, in this work we focus on *i)* the stability of the reduced basis approximation based on the Brezzi's saddle point theory and the introduction of a *supremizer* operator on the pressure terms, *ii)* a rigorous *a posteriori* error estimation procedure for velocity and pressure fields based on the Babuška's inf-sup constant (including residuals calculations), *iii)* the computation of a lower bound of the stability constant, and *iv)* different options for the reduced basis spaces construction. We present some illustrative results for both interior and external steady Stokes flows in parametrized geometries representing two parametrized classical Poiseuille and Couette flows, a channel contraction and a simple flow control problem around a curved obstacle.

Gianluigi Rozza · D.B. Phuong Huynh
Department of Mechanical Engineering and Center for Computational Engineering
MIT - Massachusetts Institute of Technology, 77 Massachusetts Ave, Cambridge, MA 02139 USA

Gianluigi Rozza · Andrea Manzoni
CMCS - Modelling and Scientific Computing
MATHICSE - Mathematics Institute of Computational Science and Engineering
EPFL - Ecole Polytechnique Fédérale de Lausanne, Station 8, CH-1015 Lausanne, Switzerland,
E-mail: gianluigi.rozza@epfl.ch, huynh@mit.edu, andrea.manzoni@epfl.ch

1 Introduction

A large set of engineering problems involve the solution of partial differential equations (PDEs), or the evaluation of some *outputs* of interest depending on a PDE solution. When a significant reduction of the marginal computational time for a single solution or output evaluation is needed, some model reduction techniques have to be taken into account; this requirement can arise both in a many-query (e.g. optimal control, parameter estimation, shape optimization) framework or in a real-time simulation context. The reduced basis (RB) method is ideally suited for the rapid and reliable solution of parametrized PDEs, i.e. PDEs depending on a set of *input* parameters which identify a given configuration of the system representing physical properties or geometrical variables.
The basic ingredients of the RB method are *i)* a rapidly convergent global approximation (Galerkin projection) onto a space spanned by solution of the governing PDE at some selected parameter values; *ii)* rigorous a posteriori error estimation procedures (inexpensive yet sharp bounds for the error in the RB field variables or output approximations); *iii)* Offline/Online computational procedures (a splitting between a very extensive and parameter independent Offline stage and an inexpensive Online calculation for each new input/output evaluation). For a very comprehensive summary of the RB methodology developed so far for coercive elliptic PDEs with affine parameter dependence please see [43,30].

Introduced in the late 1970s by Almroth, Stern and Brogan in the domain of nonlinear structural analysis and further developed by Noor in the following years [28,27], the RB method has been applied firstly to viscous fluid flow and Navier Stokes equations in the 1990s [31,18,14], considering divergence-free spaces. In the past few years, this methodology has been applied to a wide range of problems including elliptic as well as parabolic and simple hyperbolic problems. More recent contributions on stable Stokes flows in parametrized domains are contained in [39,41,47,38,37,22], while a previous a posteriori error estimation framework can be found in [36]. An example of application to the solution of shape optimization problems arising in haemodynamics and dealing with Stokes flows can be found in [23,45] and previously in [37]. The RB framework has already been applied in thermo-fluid dynamics, such as steady Navier-Stokes [9,48,26,11,34,40] parametrized flows dealing with physical [9,48] and geometrical parameters [11] or heat-mass transfer problems [46]; other existing applications include potential flows [20,42], advection-diffusion [7,44] or linear elasticity equations [25]. A combination between RB method and domain decomposition techniques is the so-called *reduced basis element method*; see [22] for the Stokes case. Recently, a RB formulation for variational inequalities by a saddle point scheme has been proposed in [15].

In this paper we first review the state of the art of RB approximation for parametrized steady Stokes flows, as a paradigm of linear elliptic noncoercive problems and we extend a stability and a posteriori error analysis based on two inf-sup constants introduced by Brezzi [2,3] and Babuška [1]. In particular, we focus on approximation and algebric stability of the RB approximation [47], a rigorous a posteriori error estimation for RB field variables, the Offline-Online computational procedure, based on the affine parametric dependence [43,30], the computation of reliable lower bounds for the *inf-sup* stability constants and on a Greedy algorithm [43,30] for the construction of the RB spaces.

The original contribution of this work deals with the fact that we are jointly providing a stability study based on the role of the Brezzi's inf-sup constant in the RB context and an error analysis and certification of results based on the estimation of the Babuška's inf-sup constant in the framework of general noncoercive problems. A former contribution on a posteriori error bounds for Stokes problem in the RB context was provided by Rovas [36] using a different approach and for divergence-free spaces. A recent approach[1] has been proposed by Veroy et al. [12] based on penalty method for flows in parametrized domains, thus reporting the problem in the coercive case [35]. Moreover, a general error estimation for linear outputs is presented, discussing both compliant and noncompliant outputs [43] and introducing a suitable dual problem for the latter case.

In this work we are interested in developing error bounds for Stokes problem as a generalized noncoercive problem in order to complete a general a posteriori error analysis for the certification of RB methods, and with a special interest in the solution of PDEs in parametrized domains. Our analysis proposes a unified framework based on the residual calculations and on the estimation of lower bounds for (the coercivity and) inf-sup stability constants using the so-called Successive Constraint Method (SCM) [17] and subsequent improvements [16]. In this way the most general noncoercive problem contains as particular cases the coercive case [43] and the parametrically coercive case [30]. Compared with other techniques for the calculation of lower bounds for the inf-sup constants, we have adopted and improved (starting from [16]) the SCM technique in its natural norm formulation to have a tool which can be considered quite versatile and handy. In this particular case we consider general error bounds for velocity and pressure, as well as for linear outputs depending on these variables. Quadratic outputs will be considered in [24].

The paper is organized as follows. After this introduction, in Sec. 2-3 we address some general features on the Stokes equations and the corresponding parametrized formulation, recalling the classical finite element approximation and the Brezzi stability theory [2,3]. In Sec. 4 we review the relevant steps for the generation of the rapidly convergent global RB approximation spaces and the approximation of the solution for parametrized Stokes equations with affine parameter dependence, focusing on the corresponding stability condition for the RB approximation, satisfied by introducing the so-called supremizer operator, and on its algebric stability, obtained through a suitable Gram-Schmidt orhonormalization of the RB basis functions. Then, in Sec. 5 we present an Offline-Online computational procedure and a Greedy procedure for the RB spaces construction. In Sec. 6 we deal with the *a posteriori* error estimation for the RB solution based on the Babuška stability theory, while in Sec. 7 we address error bounds for a generic linear output. A short review of Brezzi and Babuška theories is provided in the Appendix A; details about the construction of the *a posteriori* error bounds are reviewed in the Appendix B. In Sec. 8 some numerical examples are presented, while some concluding remarks are provided in Sec. 9.

[1] Other certified and quite complex approaches have been studied in the nonlinear steady case (Navier-Stokes equations) based on the Brezzi-Rappaz-Raviart theory [4,5]. These approaches have been proposed in [26,48] and more recently in a natural norm framework [9], focusing on physical parameters (Reynolds, Prandtl, Grashof numbers). Further developments have combined physical and geometrical parameters [11,46], dealing also with time-dependent Boussinesq equations [46,19].

2 Problem Formulation

Steady Stokes equations describe the motion of an incompressible viscous flow with constant density ρ in which the (quadratic) convective term has been neglected [35,33]; they can be stated as follows:

$$\begin{cases} -\nu \Delta \mathbf{u}_o + \nabla p_o = \mathbf{f}^o & \text{in } \Omega_o \\ \nabla \cdot \mathbf{u}_o = 0 & \text{in } \Omega_o \\ \mathbf{u}_o = \mathbf{0} & \text{on } \Gamma^o_{D_0} \\ \mathbf{u}_o = \mathbf{g}^D & \text{on } \Gamma^o_{D_g} \\ -p_o \mathbf{n} + \nu \dfrac{\partial \mathbf{u}_o}{\partial \mathbf{n}} = \mathbf{g}^N & \text{on } \Gamma^o_N, \end{cases} \tag{1}$$

where $(\mathbf{u}_o, p_o)$ are the velocity and the pressure fields defined on the original domain Ω_o, for some given $\mathbf{f}^o$, $\mathbf{g}^D$, $\mathbf{g}^N$. The first equation expresses the linear momentum conservation, the second one the mass conservation; $\nu = \mu/\rho$ denotes the kinematic viscosity, μ the dynamic viscosity, and $\mathbf{f}^o = (f_1^o, f_2^o)$ a forcing term per unit mass. In what follows, we consider a partition $\partial\Omega_o = \Gamma^o_{D_0} \cup \Gamma^o_{D_g} \cup \Gamma^o_N$, homogeneous Dirichlet conditions on $\Gamma^o_{D_0}$, non-homogeneous Dirichlet conditions on $\Gamma^o_{D_g}$ and Neumann conditions on Γ^o_N, such that the Dirichlet portion is $\Gamma^o_D = \Gamma^o_{D_0} \cup \Gamma^o_{D_g}$; $\mathbf{n}$ is the normal unit vector to the boundary $\partial\Omega_o$. We denote with X_o and Q_o the spaces $(H^1_{0,\Gamma^o_D}(\Omega_o))^2$ and $L^2(\Omega_o)$ respectively, where $H^1_{0,\Gamma^o_D}(\Omega_o) = \{v \in H^1(\Omega_o) : v|_{\Gamma^o_D} = 0\}$. We introduce a lift function $L_o\mathbf{g}^D \in (H^1(\Omega_o))^2$ and denote $\hat{\mathbf{u}}_o = \mathbf{u}_o - L_o\mathbf{g}^D$, so that $\hat{\mathbf{u}}_o|_{\Gamma_D} = \mathbf{0}$; for the sake of simplicity, we still denote $\hat{\mathbf{u}}_o$ with $\mathbf{u}_o$, as no ambiguity occurs. Hence, the weak formulation of (1) reads: find $(\mathbf{u}_o, p_o) \in X_o \times Q_o$ such that, for all $\mathbf{w} \in X_o$ and $q \in Q_o$,

$$\begin{aligned} &\nu \int_{\Omega_o} \nabla \mathbf{u}_o : \nabla \mathbf{w} \; d\Omega_o - \int_{\Omega_o} p_o \, \nabla \cdot \mathbf{w} \; d\Omega_o = \int_{\Omega_o} \mathbf{f}^o \cdot \mathbf{w} \; d\Omega_o + \int_{\Gamma^o_N} \mathbf{g}^N \cdot \mathbf{w} \; d\Gamma_o + \langle F_0^o, \mathbf{w} \rangle, \\ &\int_{\Omega_o} q \, \nabla \cdot \mathbf{u}_o \; d\Omega_o = \langle G_0^o, q \rangle, \end{aligned} \tag{2}$$

where F_0^o, G_0^o are terms due to non-homogeneous Dirichlet boundary condition on $\Gamma^o_{D_g}$. We assume that the physical, original domain is made up of R mutually nonoverlapping open subdomains: $\{\Omega_o^r\}_{r=1}^R$, so that (2) can be rewritten as:

$$\begin{cases} \mathcal{A}_o(\mathbf{u}_o, \mathbf{w}) + \mathcal{B}_o(p_o, \mathbf{w}) = \langle F^o, \mathbf{w} \rangle & \forall \mathbf{w} \in X_o \\ \mathcal{B}_o(q, \mathbf{u}_o) = \langle G^o, q \rangle & \forall q \in Q_o, \end{cases} \tag{3}$$

where

$$\mathcal{A}_o(\mathbf{v}, \mathbf{w}) = \sum_{r=1}^R \int_{\Omega_o^r} \nu_{ij}^o \frac{\partial \mathbf{v}}{\partial x_i^o} \cdot \frac{\partial \mathbf{w}}{\partial x_j^o} \; d\Omega_o, \qquad \mathcal{B}_o(q, \mathbf{w}) = -\sum_{r=1}^R \int_{\Omega_o^r} q \nabla \cdot \mathbf{w} \; d\Omega_o,$$

being $1 \le i, j \le 2$, $\nu_{ij}^o = \nu \delta_{ij}$ and δ_{ij} the Kronecker symbol (summation over i, j is understood). The right-hand side is given by $\langle F^o, \mathbf{w} \rangle = \langle F_s^o, \mathbf{w} \rangle + \langle F_0^o, \mathbf{w} \rangle$, with

$$\langle F_s^o, \mathbf{w} \rangle = \sum_{r=1}^R \int_{\Omega_o^r} \mathbf{f}^o \cdot \mathbf{w} \; d\Omega_o + \sum_{r=1}^R \int_{\Gamma_N^{o,r}} \mathbf{g}^N \cdot \mathbf{w} \; d\Gamma_o,$$

$$\langle F_0^o, \mathbf{w} \rangle = -\mathcal{A}_o(L_o\mathbf{g}^D, \mathbf{w}), \qquad \langle G^o, q \rangle = -\mathcal{B}_o(q, L_o\mathbf{g}^D),$$

where $\Gamma_N^{o,r} = \partial\Omega_o^r \cap \Gamma_N^o$.

2.1 Affine geometrical parametrization

We assume that the original domain $\Omega_o = \Omega_o(\boldsymbol{\mu})$ depends on a set of $P \geq 1$ geometrical parameters $\boldsymbol{\mu} = (\mu_1, \ldots, \mu_P) \in \mathcal{D} \subset \mathbb{R}^P$, and is obtained as the image of a reference domain $\Omega = \Omega_o(\boldsymbol{\mu}_{ref})$ through piecewise affine transformations over the coarse triangulation $\{\Omega^r\}_{r=1}^R$; the more general case of both affine and nonaffine mappings is discussed in [41]. Let us suppose that original and reference subdomains can be linked via a mapping $T(\cdot;\boldsymbol{\mu}) : \Omega^r \to \Omega_o^r(\boldsymbol{\mu})$, such that $\Omega_o^r(\boldsymbol{\mu}) = T^r(\Omega^r;\boldsymbol{\mu})$, $1 \leq r \leq R$; these mappings must be individually bijective and collectively continuous, i.e. they have to fulfill the following interface condition: $T^r(\mathbf{x};\boldsymbol{\mu}) = T^{r'}(\mathbf{x};\boldsymbol{\mu})$, for all $\mathbf{x} \in \Omega^r \cap \Omega^{r'}$, $1 \leq r < r' \leq R$. In the affine case, for the r^{th} subdomain the transformation is then given by

$$T_i^r(\mathbf{x},\boldsymbol{\mu}) = C_i^r(\boldsymbol{\mu}) + \sum_{j=1}^{2} G_{ij}^r(\boldsymbol{\mu}) x_j, \quad 1 \leq i \leq 2, \tag{4}$$

for any $\boldsymbol{\mu} \in \mathcal{D}$, $\mathbf{x} \in \Omega^r$, for given translation vectors $\mathbf{C}^r : \mathcal{D} \to \mathbb{R}^2$ and linear transformation matrices $\mathbf{G}^r : \mathcal{D} \to \mathbb{R}^{2\times 2}$, $1 \leq r \leq R$. The linear transformation matrices can effect rotation, scaling and/or shear and have to be invertible. The associated Jacobians can be defined as $J^r(\boldsymbol{\mu}) = |\det(\mathbf{G}^r(\boldsymbol{\mu}))|$, $1 \leq r \leq R$; for invertible mappings they are strictly positive. The domain decomposition which allows to trace back the problem on a reference domain shall be built on (standard) triangles, elliptical triangles and general "curvy" triangles [43,45]. They admit symbolic, numerical automation and are therefore the building blocks in the rbMIT software package `rbMIT` [21] that we use for the RB computations in this work.

2.2 Parametrized Formulation of the Stokes problem

By tracing (3) back on the reference domain Ω, the problem can be written as a system of parametrized PDEs. Denoting $X = (H^1_{0,\Gamma_D}(\Omega))^2$, $Q = L^2(\Omega)$, $\|\cdot\|_X = (\cdot,\cdot)_X^{1/2}$, $\|\cdot\|_Q = (\cdot,\cdot)_Q^{1/2}$, where $(\mathbf{v},\mathbf{w})_X = (\nabla\mathbf{v},\nabla\mathbf{w})_{(L^2(\Omega))^2}$, we have the following parametrized formulation: find $(\mathbf{u}(\boldsymbol{\mu}), p(\boldsymbol{\mu})) \in X \times Q$ such that

$$\begin{cases} \mathcal{A}(\mathbf{u}(\boldsymbol{\mu}),\mathbf{w};\boldsymbol{\mu}) + \mathcal{B}(p(\boldsymbol{\mu}),\mathbf{w};\boldsymbol{\mu}) = \langle F,\mathbf{w}\rangle & \forall \mathbf{w} \in X \\ \mathcal{B}(q,\mathbf{u}(\boldsymbol{\mu});\boldsymbol{\mu}) = \langle G,q\rangle & \forall q \in Q, \end{cases} \tag{5}$$

where

$$\mathcal{A}(\mathbf{v},\mathbf{w};\boldsymbol{\mu}) = \sum_{r=1}^{R} \int_{\Omega^r} \frac{\partial \mathbf{v}}{\partial x_i} \nu_{ij}^r(\boldsymbol{\mu}) \frac{\partial \mathbf{w}}{\partial x_j} d\Omega, \qquad \mathcal{B}(q,\mathbf{w};\boldsymbol{\mu}) = -\sum_{r=1}^{R} \int_{\Omega^r} q \chi_{ij}^r(\boldsymbol{\mu}) \frac{\partial w_j}{\partial x_i} d\Omega,$$

and $\langle F,\mathbf{w}\rangle = \langle F_s,\mathbf{w}\rangle + \langle F_0,\mathbf{w}\rangle$, with

$$\langle F_s,\mathbf{w}\rangle = \sum_{r=1}^{R} \int_{\Omega^r} \mathbf{f}\cdot\mathbf{w}\ J^r(\boldsymbol{\mu}) d\Omega + \sum_{r=1}^{R} \int_{\Gamma_N^r} \mathbf{g}^N \cdot \mathbf{w}\ K^r(\boldsymbol{\mu})\ d\Gamma,$$

$$\langle F_0,\mathbf{w}\rangle = -\mathcal{A}(L\mathbf{g}^D,\mathbf{w};\boldsymbol{\mu}), \qquad \langle G,q\rangle = -\mathcal{B}(q,L\mathbf{g}^D;\boldsymbol{\mu});$$

$K^r(\boldsymbol{\mu}) = |\mathbf{G}^r(\boldsymbol{\mu})\mathbf{t}|$, r is an index related to the r-th subdomain, $\mathbf{t}$ is the tangential unit vector to the boundary and $\Gamma_N^r = \partial\Omega^r \cap \Gamma_N$. The *transformation tensors* for the bilinear viscous terms are defined as follows:

$$\nu_{ij}^r(\boldsymbol{\mu}) = (G^r(\boldsymbol{\mu}))_{ii'}^{-1} \nu_{i'j'}^o (G^r(\boldsymbol{\mu}))_{jj'}^{-1} J^r(\boldsymbol{\mu}), \quad 1 \le i, i', j, j' \le 2, \quad r = 1, ..., R, \tag{6}$$

while the tensors for *pressure and divergence forms* are:

$$\chi_{ij}^r(\boldsymbol{\mu}) = (G^r(\boldsymbol{\mu}))_{ij}^{-1} J^r(\boldsymbol{\mu}), \quad 1 \le i, j \le 2, \quad r = 1, ..., R. \tag{7}$$

Since we are considering geometrical trasformations involving stretching and/or dilatation where the normal unit vector at the inflow and at the outflow is not changing direction, and we are lifting the Dirichlet boundary conditions under a non-zero divergence condition, we may omit the use of the *Piola transformation* and rely on a simpler change of variable [41]. More involved geometrical parametrizations managed with the Piola transformation have been considered for example in [22,10]. The latter should be used when dealing with rotations, for example.
We suppose that the bilinear form $\mathcal{A}(\cdot, \cdot; \boldsymbol{\mu})$ is continuous over X:

$$\gamma_a(\boldsymbol{\mu}) = \sup_{\mathbf{v} \in X} \sup_{\mathbf{w} \in X} \frac{\mathcal{A}(\mathbf{v}, \mathbf{w}; \boldsymbol{\mu})}{\|\mathbf{v}\|_X \|\mathbf{w}\|_X} < +\infty, \quad \forall\ \boldsymbol{\mu} \in \mathcal{D} \tag{8}$$

and coercive over X:

$$\exists\ \alpha_0 > 0 :\ \alpha(\boldsymbol{\mu}) = \inf_{\mathbf{v} \in X} \frac{\mathcal{A}(\mathbf{v}, \mathbf{v}; \boldsymbol{\mu})}{\|\mathbf{v}\|_X^2} \ge \alpha_0, \quad \forall\ \boldsymbol{\mu} \in \mathcal{D}, \tag{9}$$

and that the bilinear form $\mathcal{B}(\cdot, \cdot; \boldsymbol{\mu})$ is continuous:

$$\gamma_b(\boldsymbol{\mu}) = \sup_{q \in Q} \sup_{\mathbf{w} \in X} \frac{\mathcal{B}(q, \mathbf{w}; \boldsymbol{\mu})}{\|\mathbf{w}\|_X \|q\|_Q} < +\infty, \quad \forall\ \boldsymbol{\mu} \in \mathcal{D} \tag{10}$$

and inf-sup stable over $X \times Q$, i.e.

$$\exists\ \beta_0 > 0 :\ \beta(\boldsymbol{\mu}) = \inf_{q \in Q} \sup_{\mathbf{w} \in X} \frac{\mathcal{B}(q, \mathbf{w}; \boldsymbol{\mu})}{\|\mathbf{w}\|_X \|q\|_Q} \ge \beta_0, \quad \forall\ \boldsymbol{\mu} \in \mathcal{D}. \tag{11}$$

Furthermore, if the transformation mappings are affine in the sense of (4), the bilinear forms are affinely parametrized, i.e.

$$\mathcal{A}(\boldsymbol{\mu}; \mathbf{v}, \mathbf{w}) = \sum_{q=1}^{Q_a} \Theta_a^q(\boldsymbol{\mu}) \mathcal{A}^q(\mathbf{v}, \mathbf{w}), \qquad \mathcal{B}(\boldsymbol{\mu}; q, \mathbf{w}) = \sum_{q=1}^{Q_b} \Theta_b^q(\boldsymbol{\mu}) \mathcal{B}^q(q, \mathbf{w}); \tag{12}$$

for some integers Q_a (which may be as large as $d \times d \times d \times R$) and Q_b (as large as $d \times d \times R$), where q and s are condensed indexes of i, j, r quantities and, for $1 \le r \le R$, $1 \le i, j \le 2$,

$$\Theta_a^{q(i,j,r)}(\boldsymbol{\mu}) = \nu_{ij}^r(\boldsymbol{\mu}), \qquad \mathcal{A}^{q(i,j,r)}(\mathbf{v}, \mathbf{w}) = \int_{\Omega^r} \frac{\partial \mathbf{v}}{\partial x_i} \frac{\partial \mathbf{w}}{\partial x_j} d\Omega, \tag{13}$$

$$\Theta_b^{q(i,j,r)}(\boldsymbol{\mu}) = \chi_{ij}^r(\boldsymbol{\mu}), \qquad \mathcal{B}^{q(i,j,r)}(q, \mathbf{w}) = -\int_{\Omega^r} q \frac{\partial w_i}{\partial x_j} d\Omega. \tag{14}$$

This splitting of the operators into a part which is parameter-dependent and into a part parameter-independent (defined and computed once in the reference domain) is crucial for the computational efficiency of the method.

Finally, we introduce two linear bounded functionals $l_{\mathbf{u}} : X \to \mathbb{R}$ and $l_p : Q \to \mathbb{R}$. We may then introduce our (well-posed) continuous problem: given $\boldsymbol{\mu} \in \mathcal{D}$, evaluate the scalar output of interest

$$s(\boldsymbol{\mu}) = l(\mathbf{u}(\boldsymbol{\mu}), p(\boldsymbol{\mu}); \boldsymbol{\mu}) = l_{\mathbf{u}}(\mathbf{u}(\boldsymbol{\mu}); \boldsymbol{\mu}) + l_p(p(\boldsymbol{\mu}); \boldsymbol{\mu}) \tag{15}$$

where $(\mathbf{u}(\boldsymbol{\mu}), p(\boldsymbol{\mu})) \in X \times Q$ are solution of (5).

2.3 Stability for the numerical approximation

In the numerical approximation the Stokes problem has been solved by the Galerkin-Finite Element (FE) Method; we use here $\mathbb{P}_2 - \mathbb{P}_1$ Taylor-Hood finite elements [13]. With the superscript $\mathcal{N}$ we indicate discretized quantities ($\mathcal{N}$ is the total number of degrees of freedom and a measure of the computational complexity in the Offline stage) and finite dimensional subspaces like $X^{\mathcal{N}} \subset X$ and $Q^{\mathcal{N}} \subset Q$ for velocity ($\mathbf{u}^{\mathcal{N}}(\boldsymbol{\mu})$) and pressure ($p^{\mathcal{N}}(\boldsymbol{\mu})$), respectively. Here $X^{\mathcal{N}} \subset X$, $Q^{\mathcal{N}} \subset Q$ are two sequences of (conforming) FE approximation spaces of global dimension $\mathcal{N} = \mathcal{N}_X + \mathcal{N}_Q$. The dimension of the FE spaces is thus taken large enough in order to neglect the differences $\|\mathbf{u}^{\mathcal{N}}(\boldsymbol{\mu}) - \mathbf{u}(\boldsymbol{\mu})\|_X$ and $\|p^{\mathcal{N}}(\boldsymbol{\mu}) - p(\boldsymbol{\mu})\|_Q$, so that it can be effectively considered as a "truth" approximation. Moreover, if $\mathcal{N}$ is chosen sufficiently large, $\mathcal{A}(\cdot, \cdot; \boldsymbol{\mu})$ remains continuous and coercive over $X^{\mathcal{N}}$ [33]:

$$\gamma_a^{\mathcal{N}}(\boldsymbol{\mu}) = \sup_{\mathbf{v} \in X^{\mathcal{N}}} \sup_{\mathbf{w} \in X^{\mathcal{N}}} \frac{\mathcal{A}(\mathbf{v}, \mathbf{w}; \boldsymbol{\mu})}{\|\mathbf{v}\|_X \|\mathbf{w}\|_X} \leq \gamma_a(\boldsymbol{\mu}) < +\infty, \quad \forall\, \boldsymbol{\mu} \in \mathcal{D}$$

$$\exists\, \alpha_0 > 0 : \ \alpha^{\mathcal{N}}(\boldsymbol{\mu}) = \inf_{\mathbf{v} \in X^{\mathcal{N}}} \frac{\mathcal{A}(\mathbf{v}, \mathbf{v}; \boldsymbol{\mu})}{\|\mathbf{v}\|_X^2} \geq \alpha(\boldsymbol{\mu}) \geq \alpha_0, \quad \forall\, \boldsymbol{\mu} \in \mathcal{D}, \tag{16}$$

and $\mathcal{B}(\cdot, \cdot; \boldsymbol{\mu})$ remains continuous, i.e.

$$\gamma_b^{\mathcal{N}}(\boldsymbol{\mu}) = \sup_{q \in Q^{\mathcal{N}}} \sup_{\mathbf{w} \in X^{\mathcal{N}}} \frac{\mathcal{B}(q, \mathbf{w}; \boldsymbol{\mu})}{\|\mathbf{w}\|_X \|q\|_Q} \leq \gamma_b(\boldsymbol{\mu}) < +\infty \quad \forall\, \boldsymbol{\mu} \in \mathcal{D}$$

and inf-sup stable over $X^{\mathcal{N}} \times Q^{\mathcal{N}}$, i.e. we require that the FE spaces are chosen so that the following Brezzi inf-sup condition holds: [2,3]:

$$\exists\, \beta_0 > 0 : \ \beta^{\mathcal{N}}(\boldsymbol{\mu}) = \inf_{q \in Q^{\mathcal{N}}} \sup_{\mathbf{w} \in X^{\mathcal{N}}} \frac{\mathcal{B}(q, \mathbf{w}; \boldsymbol{\mu})}{\|\mathbf{w}\|_X \|q\|_Q} \geq \beta(\boldsymbol{\mu}) \geq \beta_0, \quad \forall\, \boldsymbol{\mu} \in \mathcal{D}. \tag{17}$$

In our case $X^{\mathcal{N}} \times Q^{\mathcal{N}}$ is the space of Taylor-Hood $\mathbb{P}_2 - \mathbb{P}_1$ elements for velocity and pressure [3,13]; however, this choice is not restrictive, the whole construction keeps holding for other spaces combinations as well.

Hence, the truth FE approximation reads as follows: given $\boldsymbol{\mu} \in \mathcal{D}$, evaluate the scalar output of interest $s(\boldsymbol{\mu}) = l(\mathbf{u}(\boldsymbol{\mu}), p(\boldsymbol{\mu}); \boldsymbol{\mu}) = l_{\mathbf{u}}(\mathbf{u}^{\mathcal{N}}(\boldsymbol{\mu}); \boldsymbol{\mu}) + l_p(p^{\mathcal{N}}(\boldsymbol{\mu}); \boldsymbol{\mu})$ where $(\mathbf{u}^{\mathcal{N}}(\boldsymbol{\mu}), p^{\mathcal{N}}(\boldsymbol{\mu})) \in X^{\mathcal{N}} \times Q^{\mathcal{N}}$ are such that

$$\begin{cases} \mathcal{A}(\mathbf{u}^{\mathcal{N}}(\boldsymbol{\mu}), \mathbf{w}; \boldsymbol{\mu}) + \mathcal{B}(p^{\mathcal{N}}(\boldsymbol{\mu}), \mathbf{w}; \boldsymbol{\mu}) = \langle F, \mathbf{w} \rangle & \forall \mathbf{w} \in X^{\mathcal{N}} \\ \mathcal{B}(q, \mathbf{u}^{\mathcal{N}}(\boldsymbol{\mu}); \boldsymbol{\mu}) = \langle G, q \rangle & \forall q \in Q^{\mathcal{N}}. \end{cases} \tag{18}$$

Our RB approximation will be built upon, and the error in our RB approximation will be measured with respect to, the truth FE approximation. In order to verify

the Brezzi inf-sup condition (17) let us introduce the following (inner, pressure) supremizer operator $T_p^{\boldsymbol{\mu}}$: $Q^{\mathcal{N}} \to X^{\mathcal{N}}$ defined as follows[2]:

$$(T_p^{\boldsymbol{\mu}} q, \mathbf{w})_X = \mathcal{B}(q, \mathbf{w}; \boldsymbol{\mu}), \quad \forall\ \mathbf{w} \in X^{\mathcal{N}}. \tag{19}$$

From this definition it is straightforward to prove that

$$T_p^{\boldsymbol{\mu}} q = \arg \sup_{\mathbf{w} \in X^{\mathcal{N}}} \frac{\mathcal{B}(q, \mathbf{w}; \boldsymbol{\mu})}{\|\mathbf{w}\|_X} \tag{20}$$

and, furthermore[3]

$$(\beta^{\mathcal{N}}(\boldsymbol{\mu}))^2 = \inf_{q \in Q^{\mathcal{N}}} \frac{(T_p^{\boldsymbol{\mu}} q, T_p^{\boldsymbol{\mu}} q)_X}{\|q\|_Q^2}. \tag{21}$$

Note from our affine assumption it follows that, for any $\varphi \in Q^{\mathcal{N}}$, the (inner, pressure) supremizer operator can be expressed as

$$T_p^{\boldsymbol{\mu}} \varphi = \sum_{q=1}^{Q_b} \Theta_b^q(\boldsymbol{\mu}) T_p^q \varphi, \tag{22}$$

where $(T_p^q \varphi, \mathbf{v})_X = \mathcal{B}^q(\varphi, \mathbf{v})$, $\forall \mathbf{v} \in X^{\mathcal{N}}$, $1 \le q \le Q_b$.

3 Reduced basis approximation: formulation and main features

The RB method efficiently computes an approximation of $(\mathbf{u}^{\mathcal{N}}(\boldsymbol{\mu}), p^{\mathcal{N}}(\boldsymbol{\mu}))$ by using global approximation spaces made up of well-chosen solutions of (18), i.e. corresponding to specific choices of the parameter values. The basic assumption is that the solution to (5) depends smoothly on the parameters, whence the parametric manifold of solutions in $X \times Q$ is smooth too and can be approximated by selecting, among classical FE solutions, some "snapshot" solutions. Let us take a relatively small set of parameter values $S_N = \{\boldsymbol{\mu}^1, \ldots, \boldsymbol{\mu}^N\}$ and consider the corresponding FE solutions $(\mathbf{u}^{\mathcal{N}}(\boldsymbol{\mu}^1), p^{\mathcal{N}}(\boldsymbol{\mu}^1)), \ldots, (\mathbf{u}^{\mathcal{N}}(\boldsymbol{\mu}^N), p^{\mathcal{N}}(\boldsymbol{\mu}^N))$, where typically $N \ll \mathcal{N}$.

We define the *reduced basis pressure space* $Q_N^{\mathcal{N}} \subset Q^{\mathcal{N}}$ as

$$Q_N^{\mathcal{N}} = \text{span}\{\xi_n := p^{\mathcal{N}}(\boldsymbol{\mu}^n),\ n = 1, \ldots, N\}.$$

The *reduced basis velocity space* $X_N^{\mathcal{N}, \boldsymbol{\mu}} \subset X^{\mathcal{N}}$ can be built as

$$X_N^{\mathcal{N}, \boldsymbol{\mu}} = \text{span}\{\zeta_n := \mathbf{u}^{\mathcal{N}}(\boldsymbol{\mu}^n),\ T_p^{\boldsymbol{\mu}} \xi_n,\ n = 1, \ldots, N\}. \tag{23}$$

[2] The pedix p stands for pressure to underline on which term the supremizer operator is acting on [41,47].

[3] In fact, (19), gives $\|T_p^{\boldsymbol{\mu}} q\|_X^2 = (T_p^{\boldsymbol{\mu}} q, T_p^{\boldsymbol{\mu}} q)_X = \mathcal{B}(q, T^{\boldsymbol{\mu}} q; \boldsymbol{\mu})$; moreover, for any $\mathbf{w} \in X^{\mathcal{N}}$

$$\frac{\mathcal{B}(q, \mathbf{w}; \boldsymbol{\mu})}{\|\mathbf{w}\|_X} = \frac{(T_p^{\boldsymbol{\mu}} q, \mathbf{w})_X}{\|\mathbf{w}\|_X} \le \frac{\|T_p^{\boldsymbol{\mu}} q\|_X \|\mathbf{w}\|_X}{\|\mathbf{w}\|_X} \le \|T_p^{\boldsymbol{\mu}} q\|_X$$

by Cauchy-Schwarz inequality, so that the following relationship holds:

$$\beta^{\mathcal{N}}(\boldsymbol{\mu}) = \inf_{q \in Q^{\mathcal{N}}} \left(\frac{1}{\|q\|_Q} \left(\sup_{\mathbf{w} \in X^{\mathcal{N}}} \frac{\mathcal{B}(q, \mathbf{w}; \boldsymbol{\mu})}{\|\mathbf{w}\|_X} \right) \right) \overset{\mathbf{w} = T_p^{\boldsymbol{\mu}} q}{=} \inf_{q \in Q^{\mathcal{N}}} \frac{\|T_p^{\boldsymbol{\mu}} q\|_X}{\|q\|_Q},$$

or, equivalently, (20).

By using Galerkin projection onto $X_N^{\mathcal{N},\boldsymbol{\mu}} \times Q_N^{\mathcal{N}}$ we obtain the following reduced basis approximation: find $(\mathbf{u}_N^{\mathcal{N}}(\boldsymbol{\mu}), p_N^{\mathcal{N}}(\boldsymbol{\mu})) \in X_N^{\mathcal{N},\boldsymbol{\mu}} \times Q_N^{\mathcal{N}}$ such that

$$\begin{cases} \mathcal{A}(\mathbf{u}_N^{\mathcal{N}}(\boldsymbol{\mu}), \mathbf{w}; \boldsymbol{\mu}) + \mathcal{B}(p_N^{\mathcal{N}}(\boldsymbol{\mu}), \mathbf{w}; \boldsymbol{\mu}) = \langle F, \mathbf{w} \rangle & \forall\ \mathbf{w} \in X_N^{\mathcal{N},\boldsymbol{\mu}} \\ \mathcal{B}(q, \mathbf{u}_N^{\mathcal{N}}(\boldsymbol{\mu}); \boldsymbol{\mu}) = \langle G, q \rangle & \forall\ \ q \in Q_N^{\mathcal{N}}; \end{cases} \tag{24}$$

consequently, our output of interest can be evaluated as

$$s_N(\boldsymbol{\mu}) = l_{\mathbf{u}}(\mathbf{u}_N^{\mathcal{N}}(\boldsymbol{\mu}); \boldsymbol{\mu}) + l_p(p_N^{\mathcal{N}}(\boldsymbol{\mu}); \boldsymbol{\mu}); \tag{25}$$

suitable corrections to (25) in order to improve accuracy will be considered in Sec. 7. Problem (24) is subject to an equivalent Brezzi reduced basis inf-sup condition [2,3]. By defining

$$\beta_N(\boldsymbol{\mu}) = \inf_{q \in Q_N^{\mathcal{N}}} \sup_{\mathbf{w} \in X_N^{\mathcal{N},\boldsymbol{\mu}}} \frac{\mathcal{B}(q, \mathbf{w}; \boldsymbol{\mu})}{\|\mathbf{w}\|_X \|q\|_Q} \tag{26}$$

the following inequalities hold:

$$\beta_N(\boldsymbol{\mu}) \geq \beta^{\mathcal{N}}(\boldsymbol{\mu}) \geq \beta_0 > 0, \qquad \forall \boldsymbol{\mu} \in \mathcal{D}, \tag{27}$$

where $\beta^{\mathcal{N}}(\boldsymbol{\mu})$ and β_0 are the same constants as in (11) and (17). In fact, recalling [39,47], we have that

$$\begin{aligned} \beta^{\mathcal{N}}(\boldsymbol{\mu}) = \inf_{q \in Q^{\mathcal{N}}} \sup_{\mathbf{w} \in X^{\mathcal{N}}} \frac{\mathcal{B}(q, \mathbf{w}; \boldsymbol{\mu})}{\|\mathbf{w}\|_X \|q\|_Q} \leq \inf_{q \in Q_N^{\mathcal{N}}} \sup_{\mathbf{w} \in X^{\mathcal{N}}} \frac{\mathcal{B}(q, \mathbf{w}; \boldsymbol{\mu})}{\|\mathbf{w}\|_X \|q\|_Q} = \\ \inf_{q \in Q_N^{\mathcal{N}}} \frac{\mathcal{B}(q, T_p^{\boldsymbol{\mu}} q; \boldsymbol{\mu})}{\|T_p^{\boldsymbol{\mu}} q\|_X \|q\|_Q} \leq \inf_{q \in Q_N^{\mathcal{N}}} \sup_{\mathbf{w} \in X_N^{\mathcal{N},\boldsymbol{\mu}}} \frac{\mathcal{B}(q, \mathbf{w}; \boldsymbol{\mu})}{\|\mathbf{w}\|_X \|q\|_Q} = \beta_N(\boldsymbol{\mu}), \end{aligned}$$

where we have applied the fact that $Q_N^{\mathcal{N}} \subset Q^{\mathcal{N}}$, the definition of the (inner, pressure) supremizer operator and the fact that the RB velocity space $X_N^{\mathcal{N},\boldsymbol{\mu}}$ is enriched by supremizers, respectively. We investigate in details the construction of the (inner, pressure) supremizer operator in next Sec. 4.

In order to express the problem (24) under the usual form of a saddle-point problem, we rewrite the RB velocity space $X_N^{\mathcal{N},\boldsymbol{\mu}}$ for computational convenience using the affine dependence of $\mathcal{B}(\cdot,\cdot;\boldsymbol{\mu})$ on the parameter and the relation (22):

$$X_N^{\mathcal{N},\boldsymbol{\mu}} = \text{span}\,\{\sum_{k=1}^{\overline{Q}^b} \Theta_b^k(\boldsymbol{\mu}) \boldsymbol{\sigma}_{kn},\ n = 1, \ldots, 2N\}, \tag{28}$$

where $\overline{Q}^b = Q^b + 1, \Theta_b^{\overline{Q}^b} = 1$ and, for $n = 1, \ldots, N$,

$$\boldsymbol{\sigma}_{kn} = 0, \quad k = 1, \ldots, Q^b; \qquad \boldsymbol{\sigma}_{\overline{Q}^b n} = \zeta_n = \mathbf{u}^{\mathcal{N}}(\boldsymbol{\mu}^n), \tag{29}$$

while, for $n = N+1, \ldots, 2N$ (in order to take account of the supremizer operator),

$$(\boldsymbol{\sigma}_{kn}, \mathbf{w})_X = \mathcal{B}^k(\xi_{n-N}, \mathbf{w}),\ \forall \mathbf{w} \in X^{\mathcal{N}}, \quad k = 1, \ldots, Q^b; \qquad \boldsymbol{\sigma}_{\overline{Q}^b n} = 0. \tag{30}$$

Hence, for a new parameter value $\boldsymbol{\mu}$, the RB solution can be written as a combination of previously computed stored solutions as basis functions:

$$\mathbf{u}_N(\boldsymbol{\mu}) = \sum_{j=1}^{2N} u_{Nj}(\boldsymbol{\mu}) \Big(\sum_{k=1}^{\overline{Q}^b} \Theta_b^k(\boldsymbol{\mu}) \boldsymbol{\sigma}_{kj} \Big), \qquad p_N(\boldsymbol{\mu}) = \sum_{l=1}^{N} p_{Nl}(\boldsymbol{\mu}) \xi_l,$$

whose weights u_{Nj} and p_{Nl} are given by the following RB linear system (in this case summation over i and j is no more understood):

$$\begin{cases} \sum_{j=1}^{2N} \sum_{q=1}^{Q_a} \Theta_a^q(\boldsymbol{\mu})\, A_{ij}^q(\boldsymbol{\mu}) u_{Nj}(\boldsymbol{\mu}) + \sum_{l=1}^{N} \sum_{q=1}^{Q_b} \Theta_b^q(\boldsymbol{\mu})\, B_{il}^q(\boldsymbol{\mu}) p_{Nl}(\boldsymbol{\mu}) = F_i(\boldsymbol{\mu}), \\ \sum_{j=1}^{2N} \sum_{q=1}^{Q_b} \Theta_b^q(\boldsymbol{\mu})\, B_{jl}^q(\boldsymbol{\mu}) u_{Nj}(\boldsymbol{\mu}) = G_l(\boldsymbol{\mu}) \end{cases} \tag{31}$$

for $1 \leq i, j \leq 2N$, $1 \leq l \leq N$, where

$$A_{ij}^q(\boldsymbol{\mu}) = \sum_{k'=1}^{\overline{Q}^b} \sum_{k''=1}^{\overline{Q}^b} \Theta_b^{k'}(\boldsymbol{\mu}) \Theta_b^{k''}(\boldsymbol{\mu}) \mathcal{A}^q(\boldsymbol{\sigma}_{k'i}, \boldsymbol{\sigma}_{k''j}), \quad B_{il}^q(\boldsymbol{\mu}) = \sum_{k'=1}^{\overline{Q}^b} \Theta_b^{k'}(\boldsymbol{\mu}) \mathcal{B}^q(\xi_l, \boldsymbol{\sigma}_{k'i}),$$

$$F_i(\boldsymbol{\mu}) = \sum_{k'=1}^{\overline{Q}^b} \Theta_b^{k'}(\boldsymbol{\mu}) \langle F, \boldsymbol{\sigma}_{k'i} \rangle, \quad 1 \leq i \leq 2N; \qquad G_l(\boldsymbol{\mu}) = \langle G^0, \xi_l \rangle, \quad 1 \leq l \leq N.$$

Finally, problem (31) can be written in compact form as

$$\begin{pmatrix} \underline{\mathrm{A}} & \underline{\mathrm{B}} \\ \underline{\mathrm{B}}^T & \mathbf{0} \end{pmatrix} \begin{pmatrix} \mathbf{u}_N \\ \mathbf{p}_N \end{pmatrix} = \begin{pmatrix} \mathbf{F} \\ \mathbf{G} \end{pmatrix}; \tag{32}$$

this linear system, whose unknowns are the coefficients of the linear combination of previously computed Offline solutions, has the same saddle-point structure of a FE approximation of a Stokes problem [33,35]. Hence, using reduced basis we deal with a matrix of considerably smaller dimension (of order of $N \ll \mathcal{N}$) but with full matrices (instead of sparse ones).

An important remark is related with the inner product and the norm matrix we are using in this problem: i.e. $(\nabla \mathbf{w}, \nabla \mathbf{v})_{L^2} + \lambda(\mathbf{w}, \mathbf{v})_{L^2} + (p, q)_{L^2}$, where $\mathbf{w}$ and $\mathbf{v}$ are related with velocity functions and q and p are related with pressure functions. The λ is the minimum eigenvalue of the Rayleigh quotient $(\nabla \mathbf{w}, \nabla \mathbf{v})_{L^2}/(\mathbf{w}, \mathbf{v})_{L^2}$. Finally, in order to exploit a suitable Offline/Online computational procedure for decoupling the generation and projection stages of the RB approximation, we need to express the velocity RB space $X_N^{\mathcal{N},\boldsymbol{\mu}}$ defined by (28) in a more viable way. In fact, we want to completely assemble/store the basis functions only once during the Offline stage, while for each new Online evaluation, given a parameter value $\boldsymbol{\mu}$, we want to compute only the parameter-dependent coefficients, and not assembling the supremizer solution as combination of previously computed solutions. Since the definition of the RB velocity space (28) still depends on $\boldsymbol{\mu}$ (because of the definition of the supremizer $T_p^{\boldsymbol{\mu}}$), we need a different way to express it. We address some possible, alternative constructions in the forthcoming section.

4 On algebraic and approximation stability

To keep under control the condition number of the reduced basis matrix we have applied the Gram-Schmidt (GS) orthogonalization procedure to velocity and pressure basis functions [30]. In particular, the orthonormalization procedure has been applied, separately, to our set of velocity snaphots, of supremizer snapshots and to our set of pressure snapshots, with respect to the $X = (H^1(\Omega))^2$ norm for velocity

(and supremizers) and $L^2(\Omega)$ for pressure. For velocity and pressure snapshots the procedure is standard, whereas it becomes more involved for the supremizer (computed) snapshots. In fact, referring to (30), we have for $n = N+1, \dots, 2N$:

$$(\boldsymbol{\sigma}_n, \mathbf{v})_X = \sum_{q=1}^{Q^b} \Theta_b^q(\boldsymbol{\mu})(\boldsymbol{\sigma}_{qn}, \mathbf{v})_X = \sum_{q=1}^{Q^b} \Theta_b^q(\boldsymbol{\mu}) \mathcal{B}^q(\xi_{n-N}, \mathbf{v}) \qquad \forall \mathbf{v} \in (H^1_{0,\Gamma_D}(\Omega))^2.$$

At this point we have two possibilities (referring to $n-th$ supremizer $\boldsymbol{\sigma}_n$, $n = N+1, \dots, 2N$) in applying orthonormalization:

a) a GS orthonormalization on $\boldsymbol{\sigma}_n$ done Online (since $\boldsymbol{\sigma}_n$ is dependent on $\boldsymbol{\mu}$) to obtain $\boldsymbol{\sigma}_n^{\perp}$ as new element (basis function) to enrich the RB velocity space:

$$\boldsymbol{\sigma}_n^{\perp} = \frac{P_n^{\perp}\boldsymbol{\sigma}_n}{||P_n^{\perp}\boldsymbol{\sigma}_n||} = \frac{P_n^{\perp}(\sum_{q=1}^{Q^b} \Theta_b^q(\boldsymbol{\mu})\boldsymbol{\sigma}_{qn})}{||P_n^{\perp}(\sum_{q=1}^{Q^b} \Theta_b^q(\boldsymbol{\mu})\boldsymbol{\sigma}_{qn})||},$$

where $P_n^{\perp} = I - L_{n-1}L_{n-1}^T$ and $L_i = \{\boldsymbol{\sigma}_1^{\perp}, ..., \boldsymbol{\sigma}_i^{\perp}\}$;

b) a GS orthonormalization on components $\boldsymbol{\sigma}_{qn}$ made Offline once and for all, since $\boldsymbol{\sigma}_{qn}$ are not depending on $\boldsymbol{\mu}$, to get $\boldsymbol{\sigma}_{qn}^{\perp *}$:

$$\boldsymbol{\sigma}_{qn}^{\perp *} = \frac{P_{qn}^{\perp}\boldsymbol{\sigma}_{qn}}{||P_{qn}^{\perp}\boldsymbol{\sigma}_{qn}||},$$

where $P_{qn}^{\perp} = I - L_{q(n-1)}L_{q(n-1)}^T$ and $L_{qi} = \{\boldsymbol{\sigma}_{q1}^{\perp *}, ..., \boldsymbol{\sigma}_{qi}^{\perp *}\}$.

We recall that, after orthonormalization (to achieve algebraic stability), we have to satisfy the approximation stability condition (27). But if we apply the approach *(a)* to RB spaces assembled as proposed in Section 3 – and in particular to supremizer solutions – *a priori* we may loose the guarantee of the approximation stability (heuristically we do not have any guarantee to fulfill (26)). In order to overcome this drawback, we decide to orthonormalize just using method *(a)* the pressure ξ and the velocity ζ basis functions and not the supremizer σ_n and use the approach *(b)* to orthogonalize the supremizer on its component σ_{kn} (before summation) to preserve approximation stability. To simplify this operation, we decide to build the RB velocity space in a slightly different way, as follows:

$$X_N^{\mathcal{N},\overline{\boldsymbol{\mu}}} = \text{span}\,\{\boldsymbol{\sigma}_n = \sum_{k=1}^{\overline{Q}^b} \Theta_b^k(\boldsymbol{\mu}^n)\boldsymbol{\sigma}_{kn},\ n = 1, \dots, 2N\}, \tag{33}$$

where $\overline{Q}^b = Q^b + 1$, $\Theta_b^{\overline{Q}^b} = 1$ and, for $n = 1, \dots, N$,

$$\boldsymbol{\sigma}_{kn} = 0, \quad \text{for } k = 1, \dots, Q^b, \qquad \boldsymbol{\sigma}_{\overline{Q}^b n} = \zeta_n = \mathbf{u}(\boldsymbol{\mu}^n),$$

while for $n = N+1, \dots, 2N$

$$(\boldsymbol{\sigma}_{kn}, \mathbf{w})_X = \mathcal{B}^k(\xi_{n-N}, \mathbf{w}) \ \ \forall\ \mathbf{w} \in Y, \quad \text{for } k = 1, \dots, Q^b, \qquad \boldsymbol{\sigma}_{\overline{Q}^b n} = 0.$$

This approach is based on the idea that the supremizers are built upon summation using the same $\boldsymbol{\mu}^j$ values used to store velocity $\zeta_j(\boldsymbol{\mu}^j)$ and pressure solutions $\xi_j(\boldsymbol{\mu}^j)$. The reduced basis solution is thus given by

$$\mathbf{u}_N(\boldsymbol{\mu}) = \sum_{j=1}^{2N} u_{Nj}(\boldsymbol{\mu})\Big(\sum_{k=1}^{\overline{Q}^b} \Theta_b^k(\boldsymbol{\mu}^j)\boldsymbol{\sigma}_{kj}\Big), \qquad p_N(\boldsymbol{\mu}) = \sum_{l=1}^{N} p_{Nl}(\boldsymbol{\mu})\xi_l,$$

and is obtained by solving the following system:

$$\begin{cases} \sum_{j=1}^{2N}\sum_{q=1}^{Q^a} \Theta_a^q(\boldsymbol{\mu})\, A_{ij}^q\, \mathbf{u}_{Nj}(\boldsymbol{\mu}) + \sum_{l=1}^{N}\sum_{q=1}^{Q^b} \Theta_b^q(\boldsymbol{\mu})\, B_{il}^q\, p_{Nl}(\boldsymbol{\mu}) = F_i,\ 1 \le i \le 2N, \\ \sum_{j=1}^{2N}\sum_{q=1}^{Q^b} \Theta_b^q(\boldsymbol{\mu})\, B_{jl}^q\, \mathbf{u}_{Nj}(\boldsymbol{\mu}) = G_l, \qquad\qquad 1 \le l \le N, \end{cases} \tag{34}$$

where, for $1 \le i, j \le 2N$, $1 \le l \le N$:

$$(A^q)_{ij} = \mathcal{A}^q(\boldsymbol{\sigma}_i, \boldsymbol{\sigma}_j) = \sum_{k'=1}^{\overline{Q}^b}\sum_{k''=1}^{\overline{Q}^b} \Theta_b^{k'}(\boldsymbol{\mu}^i)\Theta_b^{k''}(\boldsymbol{\mu}^j)\mathcal{A}^q(\boldsymbol{\sigma}_{k'i}, \boldsymbol{\sigma}_{k''j});$$

$$B_{il}^q = \mathcal{B}^q(\xi_l, \boldsymbol{\sigma}_i) = \sum_{k'=1}^{\overline{Q}^b} \Theta_b^{k'}(\boldsymbol{\mu}^i)\mathcal{B}^q(\xi_l, \boldsymbol{\sigma}_{k'i});$$

$$F_i = \langle F, \sigma_i\rangle = \sum_{k'=1}^{\overline{Q}^b} \Theta_b^{k'}(\boldsymbol{\mu}^i)\langle F, \boldsymbol{\sigma}_{k'i}\rangle, \qquad G_l = \langle G^0, \xi_l\rangle.$$

Note that all these quantities are now independent of $\boldsymbol{\mu}$, compared to those appearing in (31). This option is also competitive as regards the computational costs dealing with $3N \times 3N$ reduced basis matrices (32) instead of $(\overline{Q}^b+1)N \times (\overline{Q}^b+1)N$ matrix (usually $(\overline{Q}^b + 1) \gg 3$). We thus have the following computational costs to build the RB matrices, given also the supremizer components in the velocity space: $O(Q^a 4N^2)$ for sub-matrix $\underline{A}$, $O(Q^b 2N^2)$ for $\underline{B}$, $O(N)$ for $\underline{F}$ and $O(27N^3)$ for the inversion of the full RB matrix (32). Using this option we cannot rigorously demonstrate that the approximation stability is preserved (even without orthonormalization); nevertheless, after several numerical tests, we can safely argue that this option is very efficient and reasonably stable. Certified a posteriori error bounds are another proof of guaranteed stability using this approach combined with orthonormalization. In the following we are going to use this *"global supremizer"* option and indicate the RB velocity space as $X_N^{\mathcal{N}} \equiv X_N^{\mathcal{N},\overline{\boldsymbol{\mu}}}$ for the sake of simplicity. Numerical tests and comparisons about the different supremizer options[4] have been reported in previous works [41,47] for Stokes and [34,40] for Navier-Stokes equations.

5 Offline-Online computational procedure

The linear system (32) has normally a very small size (and a full structure) compared to the system that arises from standard FE discretization of (18), since (following the option *(ii)* discussed above) it consists of a set of $3N$ linear algebraic equations in $3N$ unknowns, while the FE discretization would lead to a set

[4] A different *"splitted supremizer"* option might be introduced as well (see e.g. [41,47]): this approach has the big advantage to preserve the approximation stability, to let us apply orthonormalization (method (ii)) and to preserve stability also after orthonormalization. Nevertheless, the cost for assembling and inverting the global RB matrix would still depend on the parametric complexity Q^a, Q^b of the problem, which can be rather high, above all in nonaffinely parametrized problems, where the empirical interpolation method has to be used in order to recover the affine parametric dependence.

of $\mathcal{N}$ equations in $\mathcal{N}$ unkowns. Nevertheless, the elements of $X_N^{\mathcal{N}}$ and $Q_N^{\mathcal{N}}$ are associated with the underlying FE space and thus are depending on $\mathcal{N}$.
A suitable Offline/Online decomposition strategy, based on the affine parameter dependence, enables to decouple the generation and projection stages of the RB approximation and thus to eliminate the $\mathcal{N}$ dependence. In this way, a very expensive (parameter independent) pre-processing Offline stage, performed only once, prepares the way for subsequent very inexpensive Online calculations, performed for (many) new PDEs solution or input-output evaluation afterwards.

In the *Offline stage* - performed only once - we first compute and store the basis functions $\{\boldsymbol{\sigma}_n\}_{n=1}^{2N}$, $\{\xi_l\}_{l=1}^{N}$, and form the matrices $\underline{A}^q$, $\underline{B}^q$, and the vectors $\underline{F}$, $\underline{G}$. This requires $O(Q^a 4N^2)$ for the sub-matrices $\underline{A}^q$, $O(Q^b 2N^2)$ for the sub-matrices $\underline{B}^q$ and $O(N)$ for the vectors $\underline{F}$ and $\underline{G}$. In the *Online stage* - performed many times, for each new value of $\boldsymbol{\mu}$ - we use the precomputed matrices $\underline{A}^q$, $\underline{B}^q$ to assemble the (full) $3N \times 3N$ stiffness matrix appearing in (32), with

$$\underline{A} = \sum_{q=1}^{Q_a} \Theta_a^q(\boldsymbol{\mu})\underline{A}^q, \qquad \underline{B} = \sum_{q=1}^{Q_b} \Theta_a^q(\boldsymbol{\mu})\underline{B}^q; \tag{35}$$

we then solve (34) to obtain the $u_{N_j}(\boldsymbol{\mu})$, $1 \le j \le 2N$, $p_{N_l}(\boldsymbol{\mu})$, $1 \le l \le N$ and evaluate the output approximation. The operation count for the Online stage is then $O((Q_a + Q_b)N^2)$ to assemble and $O(27N^3)$ to invert the full stiffness matrix, and $O(N)$ to evaluate the inner product for the output computation.

The crucial point is that our Online computational costs are dependent on Q_a and N, but independent of $\mathcal{N}$. Since $N \ll \mathcal{N}$, we can expect significant (orders of magnitude) speedup in the Online stage compared to the pure FE approach. This implies also that we may choose $\mathcal{N}$ very large in order to eliminate the error between the exact solution and the FE predictions without affecting the RB Online efficiency. In fact, the bigger the underlying FE system and thus $\mathcal{N}$ is chosen, the bigger the speedup by the use of the RB method in the Online stage will be. However, we should keep in mind that the Offline phase is still $\mathcal{N}$-dependent (a parallel Offline computation was proposed in [11]).

5.1 Sampling Strategy: a "Greedy" Algorithm

Let us introduce the product space $Y = X \times Q$ and denote with $\mathbf{U} \in Y$ the couple of velocity and pressure fields $\mathbf{U} = (\mathbf{u}, p)$; clearly

$$\|\mathbf{U}\|_Y := (\|\mathbf{u}\|_X^2 + \|p\|_Q^2)^{1/2}, \qquad \text{for all } \mathbf{U} = (\mathbf{u}, p) \in Y = X \times Q$$

is a norm on the product space Y, induced by the scalar product

$$(\mathbf{V}, \mathbf{W})_Y := (\mathbf{v}, \mathbf{w})_X + (p, q)_Q, \qquad \text{for all } \mathbf{U} = (\mathbf{u}, p), \mathbf{V} = (\mathbf{v}, q) \in Y = X \times Q.$$

In the same way, we indicate as $\mathbf{U}^{\mathcal{N}} = (\mathbf{u}^{\mathcal{N}}(\boldsymbol{\mu}), p^{\mathcal{N}}(\boldsymbol{\mu})) \in Y^{\mathcal{N}} = X^{\mathcal{N}} \times Q^{\mathcal{N}}$ and $\mathbf{U}_N^{\mathcal{N}} = (\mathbf{u}_N^{\mathcal{N}}(\boldsymbol{\mu}), p_N^{\mathcal{N}}(\boldsymbol{\mu})) \in Y_N^{\mathcal{N}} = X_N^{\mathcal{N}} \times Q_N^{\mathcal{N}}$ an element in the product of FE and RB spaces, respectively. The question we deal with in this section is how to choose the sample points $\boldsymbol{\mu}^n$, $1 \le n \le N$ for a given N such that the accuracy of the resulting RB approximation is maximized. The key ingredient is a rigourous, sharp and inexpensive a posteriori error bound $\Delta_N^{\mathcal{N}}(\boldsymbol{\mu})$ such that, for all $\boldsymbol{\mu} \in \mathcal{D}$ and for all N,

$$\|\mathbf{U}^{\mathcal{N}}(\boldsymbol{\mu}) - \mathbf{U}_N^{\mathcal{N}}(\boldsymbol{\mu})\|_Y = (\|\mathbf{u}^{\mathcal{N}}(\boldsymbol{\mu}) - \mathbf{u}_N^{\mathcal{N}}(\boldsymbol{\mu})\|_X^2 + \|p^{\mathcal{N}}(\boldsymbol{\mu}) - p_N^{\mathcal{N}}(\boldsymbol{\mu})\|_Q^2)^{1/2} \le \Delta_N^{\mathcal{N}}(\boldsymbol{\mu}).$$

We discuss the construction and properties of such an error estimator in detail in Sec. 6. We will now proceed to the "greedy" procedure which makes use of this a posteriori error estimate to construct hierarchical Lagrange RB approximation spaces [30,43,49]. Given a maximum RB dimension $N_{\max}$, a tolerance $\varepsilon_{\text{tol}}^{\text{RB}}$ and a training sample $\Xi_{\text{train}} \subset \mathcal{D}$ (a sufficiently rich finite training sample of n_{train} parameter points chosen using, for example, a uniform distribution on $\mathcal{D}$), we then choose at random $\boldsymbol{\mu}^1 \in \Xi_{\text{train}}$, the first sample point to be added to the Lagrange parameter samples $S_1 = \{\boldsymbol{\mu}^1\}$, and set $Q_1^{\mathcal{N}} = \text{span}\{\xi_1 := p^{\mathcal{N}}(\boldsymbol{\mu}^1)\}$, $X_1^{\mathcal{N}} = \text{span}\{\zeta_1 := \mathbf{u}^{\mathcal{N}}(\boldsymbol{\mu}^1),\ T_p^{\boldsymbol{\mu}^1}\xi_1\}$. The algorithm proceeds as follows:

```
for N = 2 : N_max
    μ^N = arg max_{μ∈Ξ_train} Δ_{N-1}^N(μ);
    ε_{N-1} = Δ_{N-1}^N(μ^N);
    if ε_{N-1} ≤ ε_tol^RB
        N_max = N − 1;
    end;
    S_N = S_{N-1} ∪ μ^N;
    Q_N^N = Q_{N-1}^N + span{ξ_N := p^N(μ^N)};
    X_N^{N,μ} = X_{N-1}^N + span{ζ_N := u^N(μ^N), T_p^{μ^N} ξ_N};
end.
```

Hence, the greedy algorithm[5] chooses at each iteration that particular candidate snapshot which is worst approximated by the projection on the "old" RB space $X_{N-1}^{\mathcal{N}} \times Q_{N-1}^{\mathcal{N}}$ and appends it to the retained snapshots. The most crucial point of this strategy is that the error is not measured by the (very expensive) "true" error $\|\mathbf{U}^{\mathcal{N}}(\boldsymbol{\mu}) - \mathbf{U}_N^{\mathcal{N}}(\boldsymbol{\mu})\|_Y$ but by the inexpensive a posteriori error bound $\Delta_N^{\mathcal{N}}(\boldsymbol{\mu})$. This permits us to perform Offline a very exhaustive search for the best sample with n_{train} very large and thus get most rapidly uniformly convergent spaces $Y_N^{\mathcal{N}}$. In fact only the winning candidate basis functions are computed and stored.

6 A posteriori error estimation for Stokes solution

In this section we deal with a posteriori error estimation in the RB context for affinely parametrized Stokes equations. The approach we address in this work takes advantage of the Babuška stability theory, which slightly differs from the more common Brezzi stability theory for saddle-point problems. The latter has been introduced for the approximation stability, while the former involves the global Stokes operator (viscous term, plus pressure-divergence terms). An alternative approach for a posteriori error estimation in the Stokes case and based on the splitting between viscous and pressure-divergence terms can be found in [36], whereas a more recent one based on a penalty method has been proposed in [12].

[5] Preliminary versions of the greedy algorithm for the Stokes problem were introduced in [39] using an error projection for velocity and pressure [13], respectively, instead of an error bound. More recent versions based on error bounds were described e.g. in [9,11].

Let us define the bilinear form $\tilde{\mathcal{A}}(\cdot,\cdot;\boldsymbol{\mu}) : Y \times Y \to \mathbb{R}$ given by

$$\tilde{\mathcal{A}}(\mathbf{V},\mathbf{W};\boldsymbol{\mu}) := \mathcal{A}(\mathbf{v},\mathbf{w};\boldsymbol{\mu}) + \mathcal{B}(p,\mathbf{w};\boldsymbol{\mu}) + \mathcal{B}(q,\mathbf{v};\boldsymbol{\mu}) \tag{36}$$

and the linear form

$$\tilde{F}(\mathbf{W}) := F(\mathbf{w}) + G(q), \tag{37}$$

where $\mathbf{V} = (\mathbf{v}, p)$ and $\mathbf{W} = (\mathbf{w}, q)$. We remark that, following the so-called Babuška stability theory, an alternative to (16)-(17) ensuring the well posedness of (18) is the following Babuška inf-sup stability condition:

$$\exists\ \tilde{\beta}^{\mathcal{N}}_{LB}(\boldsymbol{\mu}) > 0 :\ \tilde{\beta}^{\mathcal{N}}(\boldsymbol{\mu}) = \inf_{\mathbf{V}\in Y^{\mathcal{N}}} \sup_{\mathbf{W}\in Y^{\mathcal{N}}} \frac{\tilde{\mathcal{A}}(\mathbf{V},\mathbf{W};\boldsymbol{\mu})}{\|\mathbf{V}\|_Y \|\mathbf{W}\|_Y} \geq \tilde{\beta}^{\mathcal{N}}_{LB}(\boldsymbol{\mu}), \quad \forall\ \boldsymbol{\mu} \in \mathcal{D}. \tag{38}$$

The a posteriori error estimation used for Stokes problem is based on two main ingredients: the dual norm of residuals and an effective lower bound of the (parametric) stability factor, given in this case by the Babuška inf-sup constant $\tilde{\beta}^{\mathcal{N}}(\boldsymbol{\mu})$ defined in (38). Let us define the residuals $r_{\mathbf{v}}(\cdot\,;\boldsymbol{\mu})$ and $r_p(\cdot\,;\boldsymbol{\mu})$ by

$$\begin{aligned} r_{\mathbf{u}}(\mathbf{w};\boldsymbol{\mu}) &:= F(\mathbf{w}) - \mathcal{A}(\mathbf{u}^{\mathcal{N}}_N(\boldsymbol{\mu}),\mathbf{w};\boldsymbol{\mu}) - \mathcal{B}(p^{\mathcal{N}}_N(\boldsymbol{\mu}),\mathbf{w};\boldsymbol{\mu}), \\ r_p(q;\boldsymbol{\mu}) &:= G(q) - \mathcal{B}(q,\mathbf{u}^{\mathcal{N}}_N(\boldsymbol{\mu});\boldsymbol{\mu}). \end{aligned} \tag{39}$$

Note that

$$\begin{aligned} r_{\mathbf{u}}(\mathbf{w};\boldsymbol{\mu}) &= \mathcal{A}(\mathbf{e}_{\mathbf{u}}(\boldsymbol{\mu}),\mathbf{w};\boldsymbol{\mu}) + \mathcal{B}(e_p(\boldsymbol{\mu}),\mathbf{w};\boldsymbol{\mu}) && \forall\ \mathbf{w} \in X^{\mathcal{N}}, \\ r_p(q;\boldsymbol{\mu}) &= \mathcal{B}(q,\mathbf{e}_{\mathbf{u}}(\boldsymbol{\mu});\boldsymbol{\mu}) && \forall\ q \in Q^{\mathcal{N}}, \end{aligned} \tag{40}$$

where $\mathbf{e}_{\mathbf{u}}(\boldsymbol{\mu}) = \mathbf{u}^{\mathcal{N}}(\boldsymbol{\mu}) - \mathbf{u}^{\mathcal{N}}_N(\boldsymbol{\mu})$ and $e_p(\boldsymbol{\mu}) = p^{\mathcal{N}}(\boldsymbol{\mu}) - p^{\mathcal{N}}_N(\boldsymbol{\mu})$. Equivalently,

$$\tilde{r}(\mathbf{W};\boldsymbol{\mu}) = \tilde{\mathcal{A}}(\mathbf{U}^{\mathcal{N}}(\boldsymbol{\mu}) - \mathbf{U}^{\mathcal{N}}_N(\boldsymbol{\mu}),\mathbf{W};\boldsymbol{\mu}) \qquad \forall\ \mathbf{W} \in Y^{\mathcal{N}} \equiv X^{\mathcal{N}} \times Q^{\mathcal{N}}, \tag{41}$$

where $\tilde{r}(\mathbf{W};\boldsymbol{\mu}) := r_{\mathbf{u}}(\mathbf{w};\boldsymbol{\mu}) + r_p(q;\boldsymbol{\mu})$. Using the inf-sup condition (38), we have

$$\tilde{\beta}^{\mathcal{N}}(\boldsymbol{\mu})\|\mathbf{U}^{\mathcal{N}}(\boldsymbol{\mu}) - \mathbf{U}^{\mathcal{N}}_N(\boldsymbol{\mu})\|_X \leq \sup_{\mathbf{W}\in Y^{\mathcal{N}}} \frac{\mathcal{A}(\mathbf{U}^{\mathcal{N}}(\boldsymbol{\mu}) - \mathbf{U}^{\mathcal{N}}_N(\boldsymbol{\mu}),W;\boldsymbol{\mu})}{\|\mathbf{W}\|_Y},$$

so that the following result holds:

Proposition 1 *Let us denote by* $\mathbf{U}^{\mathcal{N}}(\boldsymbol{\mu})$ *and* $\mathbf{U}^{\mathcal{N}}_N(\boldsymbol{\mu})$ *the truth and the RB approximations, solving respectively* (18) *and* (24)*. The following residual-based estimation holds:*

$$\|\mathbf{U}^{\mathcal{N}}(\boldsymbol{\mu}) - \mathbf{U}^{\mathcal{N}}_N(\boldsymbol{\mu})\|_Y \leq \frac{\|\tilde{r}(\cdot;\boldsymbol{\mu})\|_{Y'}}{\tilde{\beta}^{\mathcal{N}}_{LB}(\boldsymbol{\mu})} =: \Delta^{\mathcal{N}}_N(\boldsymbol{\mu}), \qquad \forall\,\boldsymbol{\mu} \in \mathcal{D}, \tag{42}$$

where $\|r(\cdot;\boldsymbol{\mu})\|_{Y'} = \sup_{\mathbf{W}\in Y^{\mathcal{N}}} r(\mathbf{W};\boldsymbol{\mu})/\|\mathbf{W}\|_Y$ *is the dual norm of the residual and* $\tilde{\beta}^{\mathcal{N}}_{LB}(\boldsymbol{\mu})$ *is a computable lower bound for* $\tilde{\beta}^{\mathcal{N}}(\boldsymbol{\mu})$*.*

An alternative expression of the error estimator (42) is given by

$$\|\mathbf{u}^{\mathcal{N}}(\boldsymbol{\mu}) - \mathbf{u}^{\mathcal{N}}_N(\boldsymbol{\mu})\|^2_X + \|p^{\mathcal{N}}(\boldsymbol{\mu}) - p^{\mathcal{N}}_N(\boldsymbol{\mu})\|^2_Q \leq \frac{1}{(\tilde{\beta}^{\mathcal{N}}_{LB}(\boldsymbol{\mu}))^2}\left(\|r_{\mathbf{u}}(\cdot\,;\boldsymbol{\mu})\|^2_{X'} + \|r_p(\cdot\,;\boldsymbol{\mu})\|^2_{Q'}\right)$$

where

$$\|r_{\mathbf{u}}(\cdot\,;\boldsymbol{\mu})\|_{X'} = \sup_{\mathbf{w}\in X^{\mathcal{N}}} \frac{r_{\mathbf{u}}(\mathbf{w};\boldsymbol{\mu})}{\|\mathbf{v}\|_X}, \qquad\qquad \|r_p(\cdot\,;\boldsymbol{\mu})\|_{Q'} = \sup_{q\in Q^{\mathcal{N}}} \frac{r_p(q;\boldsymbol{\mu})}{\|q\|_Q}$$

are the dual norms of the residuals for the velocity and the pressure variables, respectively, such that $\|\tilde{r}(\cdot;\boldsymbol{\mu})\|^2_{Y'} = \|r_{\mathbf{u}}(\cdot\,;\boldsymbol{\mu})\|^2_{X'} + \|r_p(\cdot\,;\boldsymbol{\mu})\|^2_{Q'}$.

7 Error estimation for the linear outputs

We now build a posteriori error bounds for linear outputs of interest, making a distinction between the compliant and the more general noncompliant case; the quadratic case will be addressed in a forthcoming work [24].

7.1 Compliant case

Given the solution $(\mathbf{u}(\boldsymbol{\mu}), p(\boldsymbol{\mu}))$ to (5), in the compliant case we have $l_{\mathbf{u}}(\cdot) = F(\cdot)$, $l_p(\cdot) = G(\cdot)$, i.e. the output of interest can be written as

$$s(\boldsymbol{\mu}) = l(\mathbf{u}(\boldsymbol{\mu}), p(\boldsymbol{\mu}); \boldsymbol{\mu}) = F(\mathbf{u}(\boldsymbol{\mu})) + G(p(\boldsymbol{\mu}). \tag{43}$$

Correspondingly, the FE approximation of the output is given by

$$s^{\mathcal{N}}(\boldsymbol{\mu}) = l(\mathbf{u}^{\mathcal{N}}(\boldsymbol{\mu}), p^{\mathcal{N}}(\boldsymbol{\mu}); \boldsymbol{\mu}) = F(\mathbf{u}^{\mathcal{N}}(\boldsymbol{\mu})) + G(p^{\mathcal{N}}(\boldsymbol{\mu})), \tag{44}$$

while the RB approximation of the output, considering a suitable correction as proposed in [32] in order to improve the output accuracy, is given by

$$s_N^{\mathcal{N}}(\boldsymbol{\mu}) = l(\mathbf{u}_N^{\mathcal{N}}(\boldsymbol{\mu}), p_N^{\mathcal{N}}(\boldsymbol{\mu}); \boldsymbol{\mu}) + \tilde{r}(\mathbf{u}_N^{\mathcal{N}}(\boldsymbol{\mu}), p_N^{\mathcal{N}}(\boldsymbol{\mu}); \boldsymbol{\mu}), \tag{45}$$

and thus $s^{\mathcal{N}}(\boldsymbol{\mu}) - s_N^{\mathcal{N}}(\boldsymbol{\mu}) = r_{\mathbf{u}}(\mathbf{e}_{\mathbf{u}}(\boldsymbol{\mu}); \boldsymbol{\mu}) + r_p(e_p(\boldsymbol{\mu}); \boldsymbol{\mu})$. Thanks to the relationship

$$\begin{aligned} |s^{\mathcal{N}}(\boldsymbol{\mu}) - s_N^{\mathcal{N}}(\boldsymbol{\mu})| &\leq \sup_{\mathbf{w}\in X} \frac{r_{\mathbf{v}}(\mathbf{w};\boldsymbol{\mu})}{\|\mathbf{w}\|_X} \|\mathbf{e}_{\mathbf{v}}(\boldsymbol{\mu})\|_X + \sup_{q\in Q} \frac{r_p(q;\boldsymbol{\mu})}{\|q\|_Q} \|e_p(\boldsymbol{\mu})\|_Q \\ &= \|r_{\mathbf{v}}(\cdot;\boldsymbol{\mu})\|_{X'} \|\mathbf{e}_{\mathbf{v}}(\boldsymbol{\mu})\|_X + \|r_p(\cdot;\boldsymbol{\mu})\|_{Q'} \|e_p(\boldsymbol{\mu})\|_Q, \end{aligned}$$

and to the estimate (42) on velocity and pressure fields, the following result holds:

Proposition 2 *Let us denote by $s^{\mathcal{N}}(\boldsymbol{\mu})$ and $s_N^{\mathcal{N}}(\boldsymbol{\mu})$ the finite element and the reduced basis approximation, defined by* (44) *and* (45)*, respectively, of a linear output* (43) *in the compliant case. Then, the following error estimation holds:*

$$|s^{\mathcal{N}}(\boldsymbol{\mu}) - s_N^{\mathcal{N}}(\boldsymbol{\mu})| \leq 2 \left(\frac{\|r_{\mathbf{v}}(\cdot;\boldsymbol{\mu})\|_{X'}^2 + \|r_p(\cdot;\boldsymbol{\mu})\|_{Q'}^2}{\tilde{\beta}_{LB}^{\mathcal{N}}(\boldsymbol{\mu})} \right) := \Delta_N^{s,c}(\boldsymbol{\mu}), \qquad \forall\, \boldsymbol{\mu} \in \mathcal{D}, \tag{46}$$

7.1.1 Non-compliant case

Let us now consider the more general case where the output of interest is

$$s(\boldsymbol{\mu}) = l(\mathbf{u}(\boldsymbol{\mu}), p(\boldsymbol{\mu}); \boldsymbol{\mu}) = l_{\mathbf{u}}(\mathbf{u}(\boldsymbol{\mu}); \boldsymbol{\mu}) + l_p(p(\boldsymbol{\mu}); \boldsymbol{\mu}) \tag{47}$$

with $l_{\mathbf{u}}(\cdot;\boldsymbol{\mu}) \in X'$ and $l_p(\cdot;\boldsymbol{\mu}) \in Q'$ for all $\boldsymbol{\mu} \in \mathcal{D}$. In this case, we introduce the dual problem associated with $l(\cdot;\boldsymbol{\mu})$: find $(\boldsymbol{\psi}(\boldsymbol{\mu}), \lambda(\boldsymbol{\mu})) \in X \times Q$ such that

$$\begin{cases} \mathcal{A}(\mathbf{w}, \boldsymbol{\psi}(\boldsymbol{\mu}); \boldsymbol{\mu}) + \mathcal{B}(\lambda(\boldsymbol{\mu}), \mathbf{w}; \boldsymbol{\mu}) = -l_{\mathbf{u}}(\mathbf{w}; \boldsymbol{\mu}) & \forall\ \mathbf{w} \in X \\ \mathcal{B}(q, \boldsymbol{\psi}(\boldsymbol{\mu}); \boldsymbol{\mu}) = -l_p(q; \boldsymbol{\mu}) & \forall\ \ q \in Q, \end{cases} \tag{48}$$

where $\boldsymbol{\Psi}(\boldsymbol{\mu}) = (\boldsymbol{\psi}(\boldsymbol{\mu}), \lambda(\boldsymbol{\mu}))$ is denoted the dual (or adjoint) field. The corresponding FE approximation $\boldsymbol{\Psi}(\boldsymbol{\mu}) = (\boldsymbol{\psi}^{\mathcal{N}}(\boldsymbol{\mu}), \lambda^{\mathcal{N}}(\boldsymbol{\mu})) \in X^{\mathcal{N}}(\Omega) \times Q^{\mathcal{N}}(\Omega)$ solves

$$\begin{cases} \mathcal{A}(\boldsymbol{\Phi}, \boldsymbol{\psi}^{\mathcal{N}}(\boldsymbol{\mu}); \boldsymbol{\mu}) + \mathcal{B}(\lambda^{\mathcal{N}}(\boldsymbol{\mu}), \boldsymbol{\Phi}; \boldsymbol{\mu}) = -l_{\mathbf{u}}(\boldsymbol{\Phi}; \boldsymbol{\mu}) & \forall\ \boldsymbol{\Phi} \in X^{\mathcal{N}} \\ \mathcal{B}(\phi, \boldsymbol{\psi}^{\mathcal{N}}(\boldsymbol{\mu}); \boldsymbol{\mu}) = -l_p(\phi; \boldsymbol{\mu}) & \forall\ \ \phi \in Q^{\mathcal{N}}. \end{cases} \tag{49}$$

while the FE approximation of the output is given by

$$s^{\mathcal{N}}(\boldsymbol{\mu}) = l(\mathbf{u}^{\mathcal{N}}(\boldsymbol{\mu}), p^{\mathcal{N}}(\boldsymbol{\mu}); \boldsymbol{\mu}) = l_{\mathbf{u}}(\mathbf{u}^{\mathcal{N}}(\boldsymbol{\mu}); \boldsymbol{\mu}) + l_p(p^{\mathcal{N}}(\boldsymbol{\mu}); \boldsymbol{\mu}) \tag{50}$$

where $(\mathbf{u}^{\mathcal{N}}(\boldsymbol{\mu}), p^{\mathcal{N}}(\boldsymbol{\mu}))$ solve (18). The adjoint problem is thus subject to the same Brezzi inf-sup condition (17) of the primal problem. Its RB approximation is as follows: find $\boldsymbol{\Psi}_M^{\mathcal{N}}(\boldsymbol{\mu}) = (\boldsymbol{\psi}_M^{\mathcal{N}}(\boldsymbol{\mu}), \lambda_M^{\mathcal{N}}(\boldsymbol{\mu})) \in X_M^{\mathcal{N}} \times Q_M^{\mathcal{N}}$ such that

$$\begin{cases} \mathcal{A}(\mathbf{w}, \boldsymbol{\psi}_M^{\mathcal{N}}(\boldsymbol{\mu}); \boldsymbol{\mu}) + \mathcal{B}(\lambda_M^{\mathcal{N}}(\boldsymbol{\mu}), \mathbf{w}; \boldsymbol{\mu}) = -l_{\mathbf{u}}(\mathbf{w}; \boldsymbol{\mu}) & \forall\ \mathbf{w} \in X_M^{\mathcal{N}} \\ \mathcal{B}(q, \boldsymbol{\psi}_M^{\mathcal{N}}(\boldsymbol{\mu}); \boldsymbol{\mu}) = -l_p(q; \boldsymbol{\mu}) & \forall\ \ q \in Q_M^{\mathcal{N}}. \end{cases} \tag{51}$$

where the RB dual spaces $X_M^{\mathcal{N}}$, $Q_M^{\mathcal{N}}$ are built by means of a greedy algorithm and the dimension $M \ll \mathcal{N}$ is *a priori* different from the dimension N of the primal RB spaces. Similarly to (39), given the RB approximation of the dual fields $(\boldsymbol{\psi}_M^{\mathcal{N}}, \lambda_M^{\mathcal{N}}))$, we can introduce the errors $\mathbf{e}_v^{du}(\boldsymbol{\mu}) = \boldsymbol{\psi}^{\mathcal{N}}(\boldsymbol{\mu}) - \boldsymbol{\psi}_M^{\mathcal{N}}(\boldsymbol{\mu})$ and $e_p^{du}(\boldsymbol{\mu}) = \lambda^{\mathcal{N}}(\boldsymbol{\mu}) - \lambda_M^{\mathcal{N}}(\boldsymbol{\mu})$ and define the residuals as follows:

$$\begin{aligned} r_{\mathbf{u}}^{du}(\mathbf{w}; \boldsymbol{\mu}) &:= -l_{\mathbf{u}}(\mathbf{w}; \boldsymbol{\mu}) - \mathcal{A}(\mathbf{w}, \boldsymbol{\psi}_M^{\mathcal{N}}(\boldsymbol{\mu}); \boldsymbol{\mu}) - \mathcal{B}(\lambda_M^{\mathcal{N}}(\boldsymbol{\mu}), \mathbf{w}; \boldsymbol{\mu}), \\ r_p^{du}(q; \boldsymbol{\mu}) &:= -l_p(q; \boldsymbol{\mu}) - \mathcal{B}(q, \boldsymbol{\psi}_M^{\mathcal{N}}(\boldsymbol{\mu}); \boldsymbol{\mu}). \end{aligned} \tag{52}$$

Note that

$$\begin{aligned} r_{\mathbf{u}}^{du}(\mathbf{w}; \boldsymbol{\mu}) &= \mathcal{A}(\mathbf{e}_{\mathbf{u}}^{du}(\boldsymbol{\mu}), \mathbf{w}; \boldsymbol{\mu}) + \mathcal{B}(e_p^{du}(\boldsymbol{\mu}), \mathbf{w}; \boldsymbol{\mu}) \qquad \forall\ \mathbf{w} \in X^{\mathcal{N}}, \\ r_p^{du}(q; \boldsymbol{\mu}) &= \mathcal{B}(q, \mathbf{e}_{\mathbf{u}}^{du}(\boldsymbol{\mu}); \boldsymbol{\mu}) \qquad \forall\ q \in Q^{\mathcal{N}}; \end{aligned} \tag{53}$$

equivalently, $\tilde{r}^{du}(\mathbf{W}; \boldsymbol{\mu}) = \tilde{\mathcal{A}}(\boldsymbol{\Psi}^{\mathcal{N}}(\boldsymbol{\mu}) - \boldsymbol{\Psi}_M^{\mathcal{N}}(\boldsymbol{\mu}), \mathbf{W}; \boldsymbol{\mu})\ \forall\ \mathbf{W} \in Y^{\mathcal{N}} \equiv X^{\mathcal{N}} \times Q^{\mathcal{N}}$, where $\tilde{r}^{du}(\mathbf{W}; \boldsymbol{\mu}) := r_{\mathbf{u}}^{du}(\mathbf{w}; \boldsymbol{\mu}) + r_p^{du}(q; \boldsymbol{\mu})$. The RB approximation of the output is thus given by

$$s_N^{\mathcal{N}}(\boldsymbol{\mu}) = l(\mathbf{u}_N^{\mathcal{N}}(\boldsymbol{\mu}), p_N^{\mathcal{N}}(\boldsymbol{\mu}); \boldsymbol{\mu}) - \tilde{r}(\boldsymbol{\psi}_M^{\mathcal{N}}(\boldsymbol{\mu}), \lambda_M^{\mathcal{N}}(\boldsymbol{\mu}); \boldsymbol{\mu}) \tag{54}$$

where the adjoint correction helps improving the accuracy of the approximation. Hence, we have

$$\begin{aligned} s^{\mathcal{N}}(\boldsymbol{\mu}) - s_N^{\mathcal{N}}(\boldsymbol{\mu}) &= L(Y^{\mathcal{N}}(\boldsymbol{\mu}); \boldsymbol{\mu}) - L(Y_N(\boldsymbol{\mu}); \boldsymbol{\mu}) + r(\Psi_M(\boldsymbol{\mu}); \boldsymbol{\mu}) \\ &= L_{\mathbf{v}}(\mathbf{e}_{\mathbf{v}}(\boldsymbol{\mu}); \boldsymbol{\mu}) + L_p(e_p(\boldsymbol{\mu}); \boldsymbol{\mu}) + r(\Psi_M(\boldsymbol{\mu}); \boldsymbol{\mu}); \end{aligned}$$

thanks to (48) and (39), this expression can be also written as

$$\begin{aligned} s^{\mathcal{N}}(\boldsymbol{\mu}) - s_N^{\mathcal{N}}(\boldsymbol{\mu}) =& - a(\mathbf{e}_{\mathbf{v}}(\boldsymbol{\mu}), \boldsymbol{\psi}^{\mathcal{N}}(\boldsymbol{\mu}); \boldsymbol{\mu}) - b(\lambda^{\mathcal{N}}(\boldsymbol{\mu}), \mathbf{e}_{\mathbf{v}}(\boldsymbol{\mu}); \boldsymbol{\mu}) - b(e_p(\boldsymbol{\mu}), \boldsymbol{\psi}^{\mathcal{N}}(\boldsymbol{\mu}); \boldsymbol{\mu}) \\ &+ a(\mathbf{e}_{\mathbf{v}}(\boldsymbol{\mu}), \boldsymbol{\psi}_M(\boldsymbol{\mu}); \boldsymbol{\mu}) + b(\lambda_M(\boldsymbol{\mu}), \mathbf{e}_{\mathbf{v}}(\boldsymbol{\mu}); \boldsymbol{\mu}) + b(e_p(\boldsymbol{\mu}), \boldsymbol{\psi}_M(\boldsymbol{\mu}); \boldsymbol{\mu}) \\ =& - a(\mathbf{e}_{\mathbf{v}}(\boldsymbol{\mu}), \mathbf{e}_{\mathbf{v}}^{du}(\boldsymbol{\mu}); \boldsymbol{\mu}) - b(e_p^{du}(\boldsymbol{\mu}), \mathbf{e}_{\mathbf{v}}(\boldsymbol{\mu}); \boldsymbol{\mu}) - b(e_p(\boldsymbol{\mu}), \mathbf{e}_{\mathbf{v}}^{du}(\boldsymbol{\mu}); \boldsymbol{\mu}) \\ =& - r_{\mathbf{v}}^{du}(\mathbf{e}_{\mathbf{v}}(\boldsymbol{\mu}); \boldsymbol{\mu}) - r_p^{du}(e_p(\boldsymbol{\mu}); \boldsymbol{\mu}). \end{aligned}$$

Using the same procedure exploited in the compliant case, we obtain:

$$\begin{aligned} |s^{\mathcal{N}}(\boldsymbol{\mu}) - s_N^{\mathcal{N}}(\boldsymbol{\mu})| &\le \sup_{\mathbf{w} \in X} \frac{r_{\mathbf{v}}^{du}(\mathbf{w}; \boldsymbol{\mu})}{\|\mathbf{w}\|_X} \|\mathbf{e}_{\mathbf{v}}(\boldsymbol{\mu})\|_X + \sup_{q \in Q} \frac{r_p^{du}(q; \boldsymbol{\mu})}{\|\phi\|_Q} \|e_p(\boldsymbol{\mu})\|_Q \\ &= \|r_{\mathbf{v}}^{du}(\cdot; \boldsymbol{\mu})\|_{X'} \|\mathbf{e}_{\mathbf{v}}(\boldsymbol{\mu})\|_X + \|r_p^{du}(\cdot; \boldsymbol{\mu})\|_{Q'} \|e_p(\boldsymbol{\mu})\|_Q, \end{aligned}$$

so that the error bound is given by a combination of the dual norms of the dual residuals and the error on the primal variables. We have thus shown the following

Proposition 3 *Let us denote by* $s^{\mathcal{N}}(\boldsymbol{\mu})$ *and* $s_N^{\mathcal{N}}(\boldsymbol{\mu})$ *the finite element and the reduced basis approximation, defined by* (50) *and* (54)*, respectively, of a linear output* (47) *in the noncompliant case. Then, the following error estimation holds:*

$$|s^{\mathcal{N}}(\boldsymbol{\mu}) - s_N^{\mathcal{N}}(\boldsymbol{\mu})| \leq \Delta_N^{s,\,n}(\boldsymbol{\mu}), \qquad \forall\, \boldsymbol{\mu} \in \mathcal{D},$$

where

$$\Delta_N^{s,\,n}(\boldsymbol{\mu}) := 2 \left(\frac{\|r_{\mathbf{v}}^{du}(\cdot;\boldsymbol{\mu})\|_{X'}^2 + \|r_p^{du}(\cdot;\boldsymbol{\mu})\|_{Q'}^2}{\tilde{\beta}_{LB}^{\mathcal{N}}(\boldsymbol{\mu})} \right)^{1/2} \left(\frac{\|r_{\mathbf{v}}(\cdot;\boldsymbol{\mu})\|_{X'}^2 + \|r_p(\cdot;\boldsymbol{\mu})\|_{Q'}^2}{\tilde{\beta}_{LB}^{\mathcal{N}}(\boldsymbol{\mu})} \right)^{1/2}. \tag{55}$$

This result is the noncompliant version of (46): in fact, it extends the estimation obtained for the compliant case, since in the latter case, choosing $V_N^{\mathcal{N}} \equiv V_M^{\mathcal{N}}$ and $Q_N^{\mathcal{N}} \equiv Q_M^{\mathcal{N}}$, we have $\psi_M(\boldsymbol{\mu}) \equiv -\mathbf{v}_N(\boldsymbol{\mu})$, $\lambda_M(\boldsymbol{\mu}) = -p_N(\boldsymbol{\mu})$ and the same expression for primal and dual residuals.

8 Numerical Examples

Flows in pipes and channels or around bodies are of great interest in fluid mechanics applications [29], especially when they can be studied in a parametrized geometrical configuration. The following examples consider low Reynolds viscous flows described by 2D steady Stokes equations in different geometries; they can be seen as examples for the design of parametrized fluidic devices or considered as elements of more complex modular fluidic systems.
The computations, provided in this work as examples, have been done in five different geometrical configurations and deal with two classic Poiseuille and Couette flows, a flow in a channel contraction and around a curved bluff body. The following subsections are devoted to the description of these problems, with results showing the application of the proposed and revisited methodology. All numerical details concerning the construction of RB spaces and the computation of lower bounds $\tilde{\beta}_{LB}^{\mathcal{N}}(\boldsymbol{\mu})$ are reported in Tables 1 and 2.

8.1 Poiseuille and Couette flows

This first example deals with two classical flows in straight pipes of uniform cross-section, known as Hagen-Poiseuille and Couette flows [29]. In the former a parabolic velocity profile is imposed at the inflow, while in the latter we deal with a flow in the space between two parallels sections, one of which is moving relative to the other.
For the Poiseuille case, we consider the physical domain $\Omega_o(\mu)$ shown in Figure 1 and $P = 2$ parameters. Here $\mu_1 = \nu$ is a physical parameter, while μ_2 is a geometrical parameter representing the lenght of the right narrow channel. The parameter domain is given by $\mathcal{D} = [0.25, 0.75] \times [1.5, 2.5]$. The forcing term is $\mathbf{f} = (1, 0)$.
We impose the following boundary conditions (with $\Gamma_D \equiv \Gamma_{D_0} = \partial\Omega \setminus (\Gamma_1 \cup \Gamma_7)$):

$$\begin{array}{lll} \mathbf{u} = \mathbf{0} & & \text{on } \Gamma_D \\ u_1 = 0, \quad u_2 = 4x_1(1 - x_1) & & \text{on } \Gamma_1 \\ u_1 = 0, \quad -pn_2 + \nu \dfrac{\partial u_2}{\partial x_2} n_2 = 0 & & \text{on } \Gamma_7 \end{array} \qquad \text{(Poiseuille case)}$$

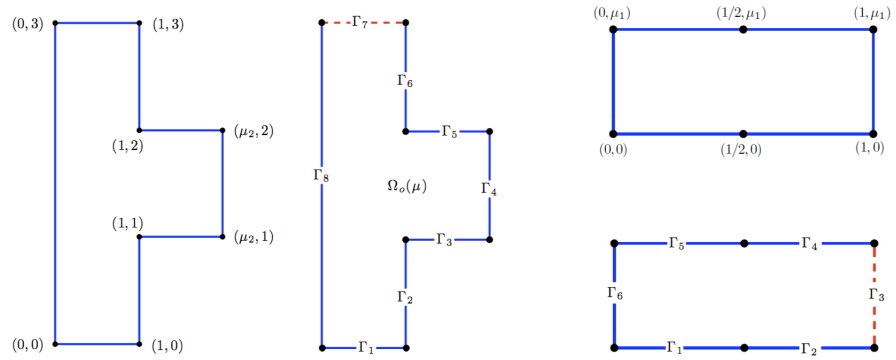

Fig. 1 Parametrized geometry and domain boundaries for the Poiseuille (left) and the Couette (right) case.

where $\mathbf{n} = (n_1, n_2)^T$ denotes the normal unit vector and $\nu = \mu_1$. For the Couette case, we consider the physical domain $\Omega_o(\mu)$ shown in Figure 1 (right side) and $P = 1$ parameter, $\mu_1 \in [0.5, 2]$, being both the height of the channel and the maximum value of the linear profile of inlet velocity prescribed. The forcing term is $\mathbf{f} = (0, -1)$. Denoting $\Gamma_D = \partial\Omega \setminus \Gamma_3$, we impose the following boundary conditions:

$$\begin{aligned} &u_1 = y, \quad u_2 = 0 && \text{on } \Gamma_D \\ &u_2 = 0, \quad -pn_1 + \frac{\partial u_1}{\partial x_1} n_1 = 0 && \text{on } \Gamma_3 \end{aligned} \qquad \text{(Couette case)}$$

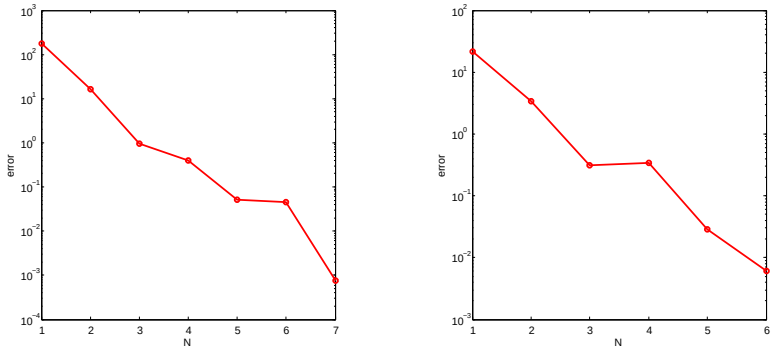

Fig. 2 Poiseuille (left) and Couette (right) cases: relative errors $\max_{\boldsymbol{\mu}\in\Xi_{train}} (\Delta_N^{\mathcal{N}}(\boldsymbol{\mu})/\|\mathbf{U}_N^{\mathcal{N}}(\boldsymbol{\mu})\|_Y)$ as a function of N for the RB approximations computed during the greedy procedure. Here Ξ_{train} is a uniform random sample of size $n_{\text{train}} = 1000$ and the RB tolerance is $\varepsilon_{\text{tol}}^{\text{RB}} = 10^{-2}$.

We show in Figure 2 the convergence of the greedy procedure for the construction of the RB spaces; with a fixed tolerance $\varepsilon_{\text{tol}}^{\text{RB}} = 10^{-2}$, $N_{max} = 7$ and $N_{max} = 6$ basis functions have been selected for the Poiseuille and the Couette cases, respectively. We also plot in Figure 3 the SCM lower and upper bounds for the Babuška inf-sup constant (e.g. for a selected value of μ_1 in the Poiseuille case, using for both the cases in the Online evaluation a uniform train sample of 1000 parameter values). For these cases the output of interest is provided by the visualization of velocity and pressure contour fields; two examples are reported in Figures 4 and 5.

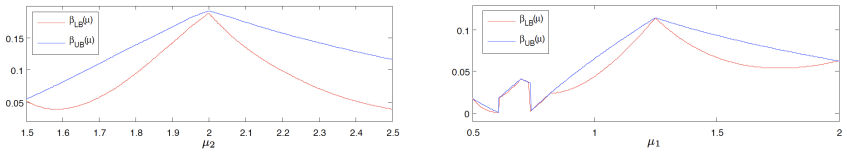

Fig. 3 Poiseuille (left) and Couette (right) cases: lower and upper bounds for the Babuška inf-sup constant; here Ξ_{train} is a uniform sample of size $n_{\text{train}} = 1000$: $\tilde{\beta}^{\mathcal{N}}_{LB}(\boldsymbol{\mu})$ (red curve) and $\tilde{\beta}^{\mathcal{N}}_{UB}(\boldsymbol{\mu})$ (blue curve) as a function of μ_2 for the Poiseuille case (being $\mu_1 = 0.5$ fixed) and of μ_1 for the Couette case after 27 and 15 iterations of the SCM greedy algorithm, respectively.

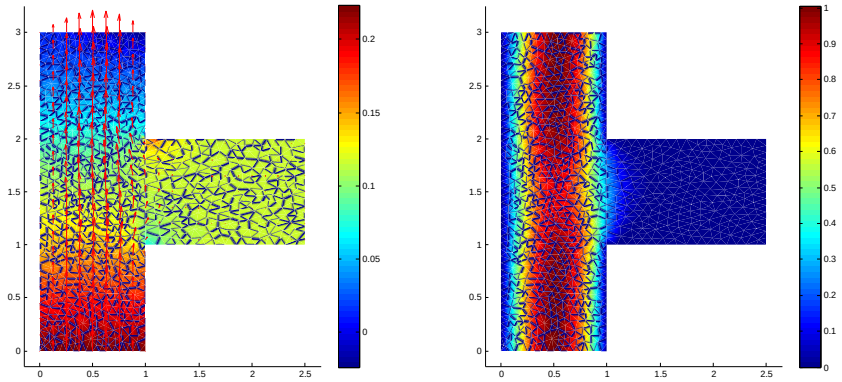

Fig. 4 Poiseuille case: representative solution for pressure with streamlines (left) and velocity (right) for $\boldsymbol{\mu} = [0.25, 2.5]$.

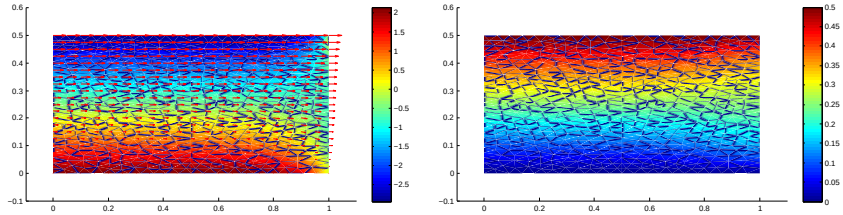

Fig. 5 Couette case: representative solution for pressure with streamlines (left) and velocity (right) for $\boldsymbol{\mu} = 0.5$.

We plot in Figure 6 the errors between the "truth" FE solution and the RB approximation, for $N = 1, \ldots, N_{max}$, and the corresponding error bounds. We remark both the rigor and the sharpness of the error bounds, being the effectivity $\eta_N(\boldsymbol{\mu}) := \Delta_N(\boldsymbol{\mu}) / \|\mathbf{U}^{\mathcal{N}}(\boldsymbol{\mu}) - \mathbf{U}^{\mathcal{N}}_N(\boldsymbol{\mu})\|_Y$ greater than 1 (rigor) and not so far from unity (sharpness).

8.2 A channel contraction

The problem of the change of a sectional area characterizes many engineering problems dealing with internal flows. The physical phenomena observed in the channel at the change of the sectional area are based on the continuity equation; another important aspect is the calculation of flow rates at a selected section

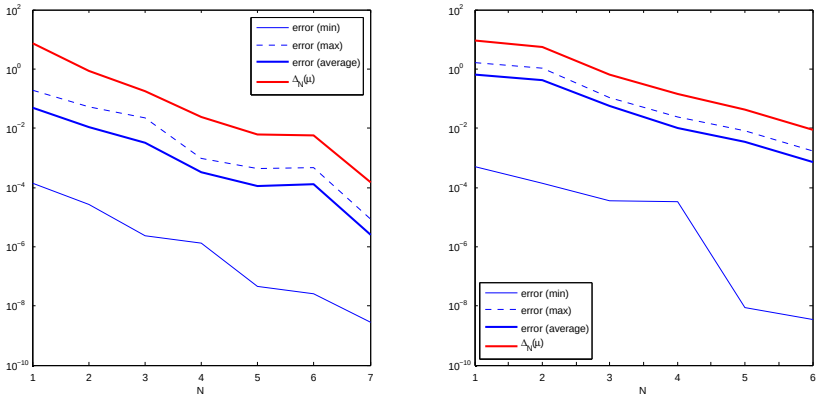

Fig. 6 Poiseuille (left) and Couette (right) cases: a posteriori error bounds and (minimum, maximum and average) computed errors between the "truth" FE solution and the RB approximation, for $N = 1, \ldots, N_{max}$. Here Ξ_{train} is a uniform sample of size $n_{\text{train}} = 1000$.

of the channel. We consider the physical domain $\Omega_o(\mu)$ shown in Figure 7; we identify the regions $\mathcal{R}_\ell$, $1 \le \ell \le 2$, which represent the portions of the channel with different sectional area. We consider $P = 3$ parameters; here μ_1, μ_2, μ_3 are geometrical parameters defined in Figure 7: μ_1 is the length of the larger zone of the channel before the contraction, μ_2 is the length of the narrow zone of the channel (just before the outflow) and μ_3 is the diameter of the channel at the inflow. The parameter domain is given by $\mathcal{D} = [3,5] \times [3,5] \times [2.5,3]$. The forcing term is $\mathbf{f} = (0,0)$. We impose the following boundary conditions:

$$\begin{aligned}
&\mathbf{u} = \mathbf{0} && \text{on } \Gamma_1, \Gamma_2, \Gamma_4, \Gamma_6, \Gamma_7, \Gamma_8 \\
&u_2 = 0, \quad -pn_1 + \frac{\partial u_1}{\partial x_1} n_1 = 1 && \text{on } \Gamma_5. \\
&u_2 = 0, \quad -pn_1 + \frac{\partial u_1}{\partial x_1} n_1 = -1 && \text{on } \Gamma_9, \Gamma_{10}, \Gamma_{11}.
\end{aligned}$$

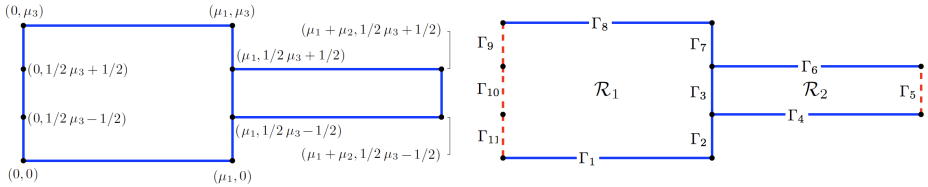

Fig. 7 Parametrized geometry and domain boundaries for the channel contraction case.

The output of interest is the flowrate on Γ_3 (internal boundary at the interface, on which the continuity of velocity and stresses is assured), given by

$$s(\boldsymbol{\mu}) = \int_{\Gamma_3} u_1(\boldsymbol{\mu}) d\Gamma.$$

We show in Figure 8 the convergence of the greedy procedure for the construction of the primal and dual RB spaces; with a fixed tolerance $\varepsilon_{\text{tol}}^{\text{RB}} = 10^{-2}$, $N_{max}^{pr} = 11$

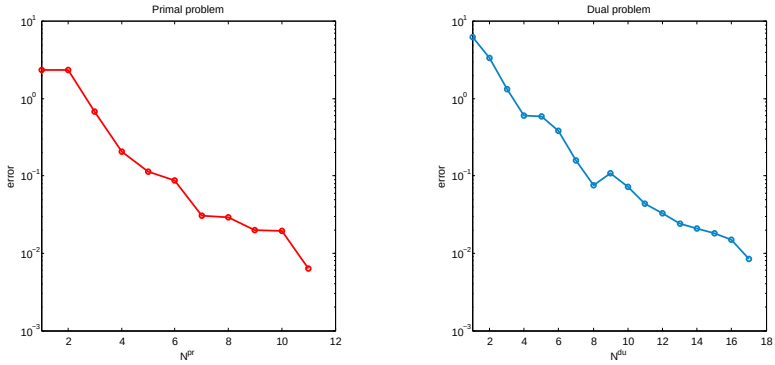

Fig. 8 Channel contraction case: relative errors $\max_{\boldsymbol{\mu}\in\Xi_{train}}(\Delta_N^{\mathcal{N}}(\boldsymbol{\mu})/\|\mathbf{U}_N^{\mathcal{N}}(\boldsymbol{\mu})\|_Y)$ and $\max_{\boldsymbol{\mu}\in\Xi_{train}}(\Delta_M^{\mathcal{N}}(\boldsymbol{\mu})/\|\boldsymbol{\Psi}_M^{\mathcal{N}}(\boldsymbol{\mu})\|_Y)$ as a function of $N = N^{pr}$ and $M = N^{du}$ for the RB approximations computed during the greedy procedure, for the primal (left) and the dual (right) problem, respectively. Here Ξ_{train} is a uniform random sample of size $n_{\text{train}} = 1000$ and the RB tolerance is $\varepsilon_{\text{tol}}^{\text{RB}} = 10^{-2}$.

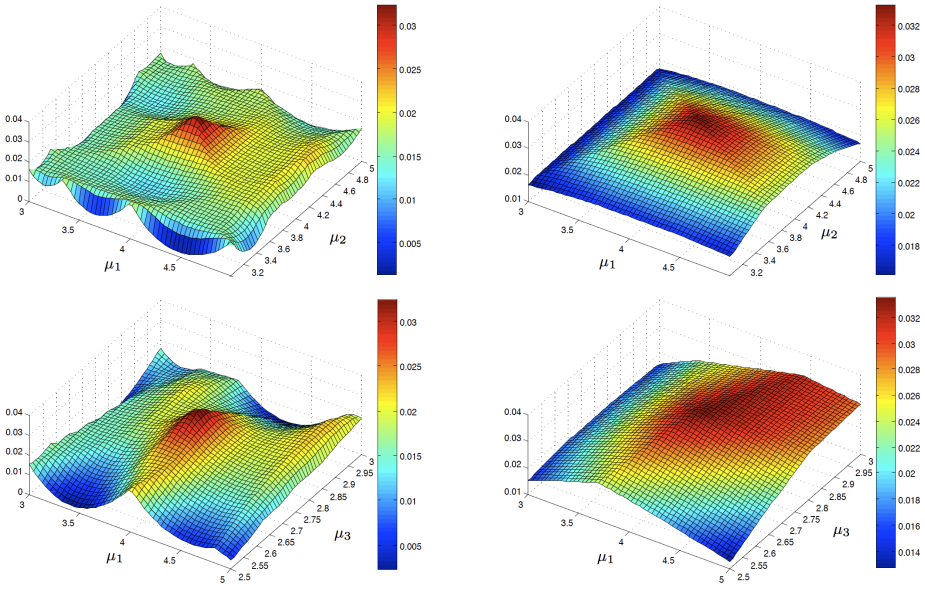

Fig. 9 Channel contraction case: lower (left) and upper (right) bounds for the Babuška inf-sup constant; here Ξ_{train} is a uniform sample of size $n_{\text{train}} = 2500$: $\tilde{\beta}_{LB}^{\mathcal{N}}(\boldsymbol{\mu})$ and $\tilde{\beta}_{UB}^{\mathcal{N}}(\boldsymbol{\mu})$ as a function of μ_1, μ_2 (top, being $\mu_3 = 2.75$ fixed) and of μ_1, μ_3 (bottom, being $\mu_2 = 4$ fixed) after 49 iterations of the SCM greedy algorithm.

and $N_{max}^{du} = 17$ basis functions have been selected for the primal and the dual problem, respectively. We also plot in Figure 9 the SCM lower and upper bounds for the Babuška inf-sup constant, using in the Online evaluation a uniform train sample of size $n_{\text{train}} = 2500$.

In Figure 10 we report some representative solutions for selected values of the parameters. In Figure 11 we plot the computed output, together with the related error bound, as functions of μ_1 and μ_2, being μ_3 fixed to its intermediate value.

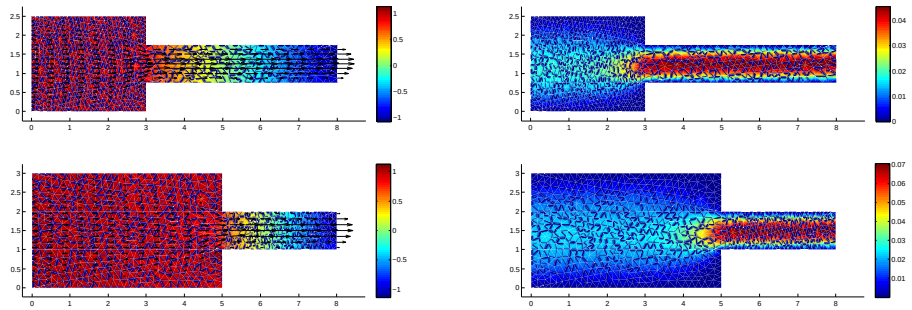

Fig. 10 Channel contraction case: representative solutions for pressure with streamlines (left) and velocity (right) for $\boldsymbol{\mu} = [3, 5, 2.5]$ and $\boldsymbol{\mu} = [5, 3, 3]$.

We recall the quadratic effect recovered by introducing and solving the dual problem in the case of a noncompliant output.

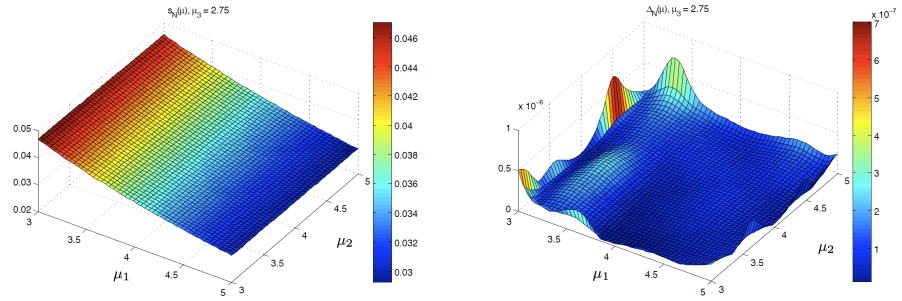

Fig. 11 Channel contraction case: computed output (left) and related error bound (right) as functions of μ_1, μ_2, with $\mu_3 = 2.75$. The average time for Online output evaluation is $0.148s$.

8.3 A curved bluff body

A common problem in fluid dynamics is the drag minimization around a body which is in relative motion in a fluid; airfoils or hull appendages in boats (at high Reynolds number) or blunt bodies in flows (at low Reynolds numbers) are just a couple of examples of applications. Here we consider a simplified version of the drag minimization problem addressed in [6], in which drag forces are minimized controlling the velocity through the body boundary. We are now interested in computing the Stokes flow and related drag forces around a profile in relative motion with a laminar viscous fluid, with respect to simple parametric variations. A complete formulation in the optimal control and shape optimization framework using RB approximation will be the object of another forthcoming work.
We consider the geometrical setting depicted in Figure 12: here $\mu_1 \in [0.1, 0.25]$ is a geometrical parameter representing the body lenght, while $\mu_2 \in [-25, 25]$ is the Neumann datum prescribed on the boundaries $\Gamma_9 \cup \Gamma_{11}$: as in [6], this corresponds to regulate the aspiration or the blowing of the boundary layer for reducing the effects of the vortices coming off from the rear of the body. The forcing term is $\mathbf{f} = (0, 0)$.

A parabolic flow is imposed at the inlet $\Gamma_7 \cup \Gamma_8$, while a free-stress condition is imposed at the outflow $\Gamma_4 \cup \Gamma_5$. Thus, we impose the following boundary conditions:

$$
\begin{aligned}
&\mathbf{u} = \mathbf{0} && \text{on } \Gamma_1, \Gamma_2, \Gamma_5, \Gamma_6, \Gamma_{10}, \Gamma_{12}, \Gamma_{13}, \\
&u_1 = \alpha(x_2 - 0.4)(x_2 + 0.4), \quad u_2 = 0 && \text{on } \Gamma_7, \Gamma_8, \\
&u_1 = 0, \quad -pn_2 + \frac{\partial u_2}{\partial x_2} n_2 = \mu_2 && \text{on } \Gamma_9, \\
&u_1 = 0, \quad -pn_2 + \frac{\partial u_2}{\partial x_2} n_2 = \mu_2 && \text{on } \Gamma_{11}, \\
&-p\mathbf{n} + \frac{\partial \mathbf{u}}{\partial \mathbf{n}} = \mathbf{0} && \text{on } \Gamma_3, \Gamma_4.
\end{aligned}
$$

where $\alpha = 0.16$ in order to have a maximum velocity at the inlet equal to 1.

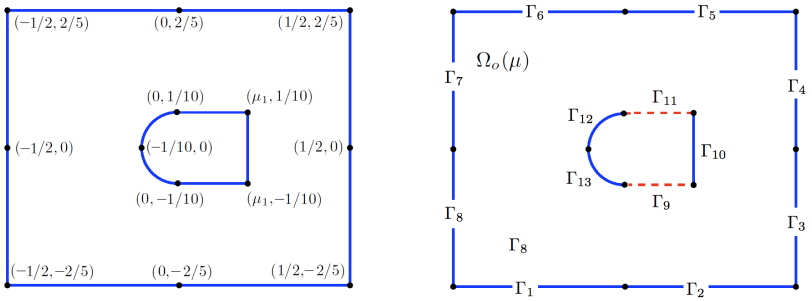

Fig. 12 Parametrized geometry and domain boundaries for the curved bluff body case.

The output of interest is the drag force acting on the Dirichlet boundary of the body $\Gamma_B = \Gamma_{10} \cup \Gamma_{12} \cup \Gamma_{13}$, given by

$$
s(\boldsymbol{\mu}) = \int_{\Gamma_B} \left(p\mathbf{n} - \frac{\partial \mathbf{u}}{\partial \mathbf{n}} \right) \cdot \hat{\mathbf{u}}_D d\Gamma,
$$

where $\hat{\mathbf{u}}_D = (1, 0)$ is the direction of the inflow velocity. We show in Figure 13 the convergence of the greedy procedure for the construction of the primal and dual RB spaces; with a fixed tolerance $\varepsilon_{\text{tol}}^{\text{RB}} = 10^{-2}$, $N_{max}^{pr} = 12$ and $N_{max}^{du} = 6$ basis functions have been selected for the primal and the dual problem, respectively.

We also plot in Figure 14 the SCM lower and upper bounds for the inf-sup constant; clearly, they do not depend on μ_2, which does not affect the left-hand-side of the Stokes operator. In Figure 15 we report some representative solutions for selected values of the parameters. We can underline a strong sensitivity of the flow with respect to geometrical variations and, clearly, also on the aspiration/blowing of the fluid across the body. In Figure 16 we plot the computed output, together with the related error bound. The output behaves as a non-monotonic function w.r.t. the two parameters. There is a different influence of the bluff body geometry (i.e. short or long body) w.r.t. the shear layers and the separation.

We plot in Figure 17 the errors between the "truth" FE solution and the RB approximation, for $N = 1, \ldots, N_{max}$, and the corresponding error bounds.

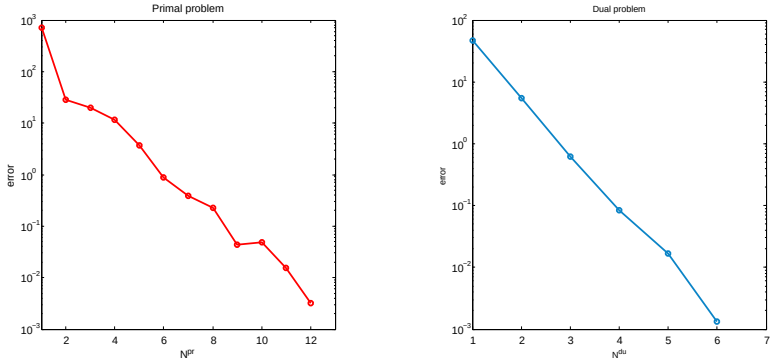

Fig. 13 Curved bluff body case: relative errors $\max_{\boldsymbol{\mu}\in\Xi_{train}}(\Delta_N^{\mathcal{N}}(\boldsymbol{\mu})/\|\mathbf{U}_N^{\mathcal{N}}(\boldsymbol{\mu})\|_Y)$ and $\max_{\boldsymbol{\mu}\in\Xi_{train}}(\Delta_M^{\mathcal{N}}(\boldsymbol{\mu})/\|\boldsymbol{\Psi}_M^{\mathcal{N}}(\boldsymbol{\mu})\|_Y)$ as a function of $N = N^{pr}$ and $M = N^{du}$ for the RB approximations computed during the greedy procedure, for the primal (left) and the dual (right) problem, respectively. Here Ξ_{train} is a uniform random sample of size $n_{\text{train}} = 1000$ and the RB tolerance is $\varepsilon_{\text{tol}}^{\text{RB}} = 10^{-2}$.

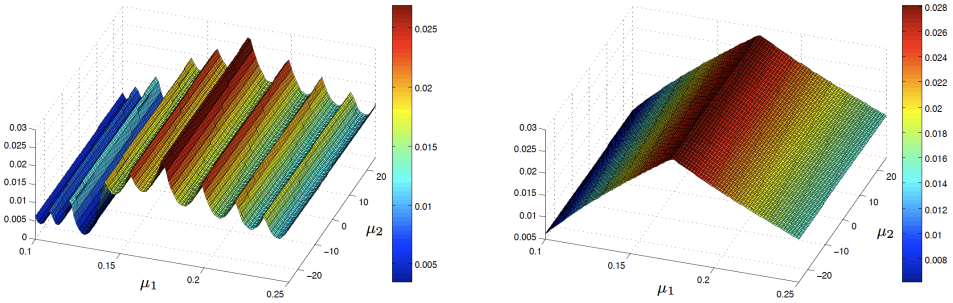

Fig. 14 Curved bluff body case: lower and upper bounds for the Babuška inf-sup constant; here Ξ_{train} is a uniform sample of size $n_{\text{train}} = 2500$: $\tilde{\beta}_{LB}^{\mathcal{N}}(\boldsymbol{\mu})$ and $\tilde{\beta}_{UB}^{\mathcal{N}}(\boldsymbol{\mu})$ as a function of μ_1, μ_2 after 10 iterations of the SCM greedy algorithm.

8.4 Summary results

We report all the details of the numerical simulations related to the discussed test cases in Table 1. We remark the very small dimension N of the RB approximation problems with respect to the FE approximation space dimension $\mathcal{N}$, which leads to effective computational economies, necessary when dealing with numerical simulations in both real time and many query context. The reduction in linear systems dimension is about between 200 and 400 times, depending on the test cases, while the computational speedup is of order 10^2, varying from 98 to 442. Computational time for Online evaluation is of order 10^{-2} seconds. The natural norm SCM algorithm enables to contain the computational costs arising from the computation of the lower bound of the inf-sup constant, also in the cases of larger parameter spaces $\mathcal{D}$, as for the curved bluff body case (see Table 2).

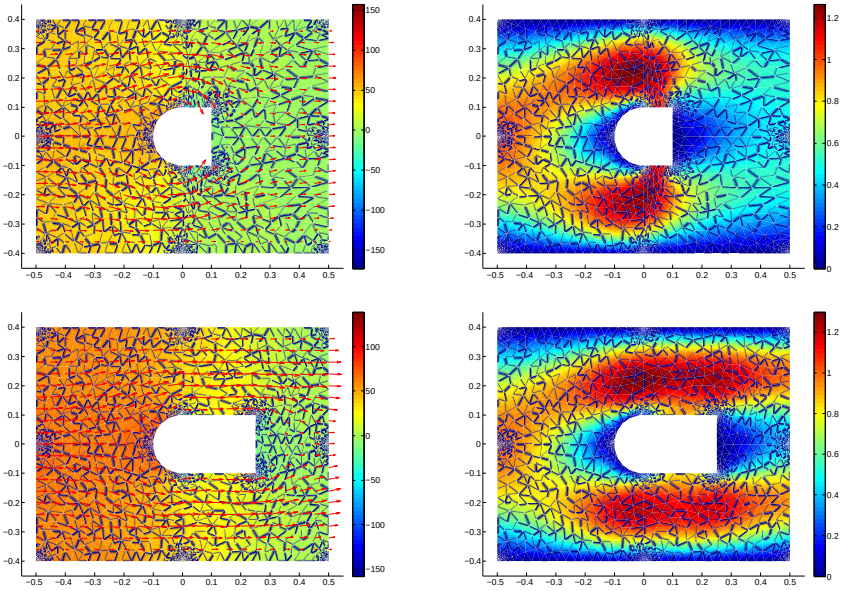

Fig. 15 Curved bluff body case: representative solutions for pressure with streamlines (left) and velocity (right) for $\boldsymbol{\mu} = [0.1, -25]$ (top) and $\boldsymbol{\mu} = [0.25, 25]$ (bottom).

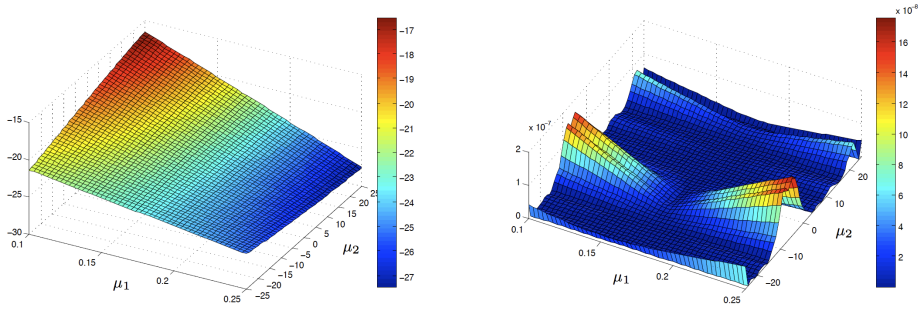

Fig. 16 Curved bluff body case: computed output (left) and related error bound (right) as a function of μ_1, μ_2. The average time for Online output evaluation is $0.087s$.

9 Conclusions

We have investigated the role of the inf-sup constants in parametrized Stokes equations solved by reduced basis method. The stability of the RB methodology is guaranteed through an equivalent Brezzi's inf-sup constant, while the certified error bounds on velocity and pressure have been proposed by considering a parametrized Babuska's inf-sup constant (and its lower bound computed by a linear programming algorithm (SCM)). Several numerical tests have proved the computational efficiency and the reliability of the proposed methodology. Further developments will be devoted in the treatment of quadratic outputs in view of optimal control and shape optimization problems.

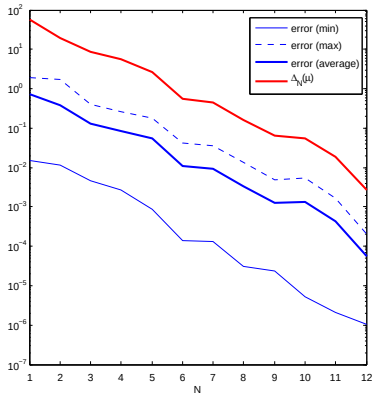

Fig. 17 Curved bluff body case: a posteriori error bounds and (minimum, maximum and average) computed errors between the "truth" FE solution and the RB approximation, for $N = 1, \ldots, N_{max}$. Here Ξ_{train} is a uniform sample of size $n_{\text{train}} = 500$.

Approximation data	Poiseuille	Couette	Contraction	Body
Number of parameters P	2	1	3	2
Affine op. components $Q_a + 2Q_b$	5	3	8	8
Affine rhs components Q_f	2	4	2	9
FE space dim. $\mathcal{N}$	8354	5093	6490	13216
RB primal space dim. N^{pr}_{max}	7	6	11	12
RB dual space dim. N^{du}_{max}	-	-	17	6
FE evaluation t^{online}_{FE} (s)	3.987	2.005	3.464	10.483
RB evaluation t^{online}_{RB} (s)	0.0101	0.0205	0.0212	0.0237
Computational speedup	395	98	163	442

Table 1 Numerical details for the test cases presented. RB spaces have been built by means of the greedy procedure, using a tolerance $\varepsilon^{\text{RB}}_{\text{tol}} = 10^{-2}$ and a uniform RB greedy train sample of size $n_{\text{train}} = 1000$. A comparison of the computational times between the Online RB evaluations and the corresponding FE simulations is reported. Here t^{online}_{RB} is the time of an Online RB computation, while t^{online}_{FE} is the time for a FE computation, once FE matrices are built.

Approximation data	Poiseuille	Couette	Contraction	Body
Number of selected $\bar{\boldsymbol{\mu}}$	2	3	1	1
Number of selected $\hat{\boldsymbol{\mu}}$ ($\forall \bar{\boldsymbol{\mu}}$)	22; 5	7; 5; 3	49	10
Number of eigenproblems	39	24	66	27

Table 2 Numerical details for the test cases presented. The lower and upper bounds of the Babuška inf-sup constants have been computed by means of the natural norm SCM algorithm detailed in [16], using a tolerance $\varepsilon^{SCM}_{\text{tol}} = 0.85$ and a uniform train sample of size $n_{\text{train}} = 1000$. SCM requires the solution of $\#\bar{\boldsymbol{\mu}} + \#\hat{\boldsymbol{\mu}} + 2(Q_a + 2Q_b)$ eigenproblems.

Acknowledgements

We acknowledge Prof. A. Quarteroni for his support and insights, Prof. A.T. Patera (MIT) for contributions and encouragement, as well as all the people who have contributed to the `rbMIT` package (beta version) used for RB computations presented in this work. In particular, we thank Dr. N.C. Nguyen (MIT) and Dr. T. Lassila (Aalto University) for their feedbacks and suggestions.

This work has been supported in part by the Swiss National Science Foundation (Project 200021-122136), by the ERC-Mathcard Project (Project ERC-2008-AdG 227058) and by the Progetto Roberto Rocca (MIT-Politecnico di Milano) and the AFOSR (Grant No. FA9550-07-1-0425 and OSD/AFOSR Grant No. FA9550-09-1-0613).

Appendix A: On the relationship between Brezzi and Babuška theories

In this short section we report some observations on the two inf-sup stability theories formulated by Babuška [1] and Brezzi [2], briefly discussing the relationship between the two theories and underlining the motivations on which we have based and developed the previous analysis. Some recent contributions, on which this section is based, can be found in the works by Xu and Zikatanov [50] and Demkowicz [8]. Considering a continuous bilinear form $\Phi(\cdot,\cdot) : U \times V \to \mathbb{R}$, the Babuška theory states that the problem[6]

$$\text{find} \quad y \in U : \quad \Phi(y,z) = \langle f, z\rangle \qquad \forall\ z \in V$$

is well posed if and only inf the following (Babuška) inf-sup condition holds:

$$\inf_{y\in U}\sup_{z\in V}\frac{\Phi(y,z)}{\|y\|_U\|z\|_V} = \inf_{z\in V}\sup_{y\in U}\frac{\Phi(y,z)}{\|y\|_U\|z\|_V} = \beta_{BA} > 0, \tag{56}$$

and the unique solution of (36) satisfies

$$\|y\|_U \le \frac{\|f\|_{V^*}}{\beta_{BA}}. \tag{57}$$

In this way, the Babuška theory can be seen as a generalization to the Petrov-Galerkin case of the Lax-Milgram result for the Galerkin-type formulation; its application to the Stokes problem is just a possible use. Our interest is to create a general framework to compute error bounds for noncoercive problems solved by reduced basis. On the other hand, the Brezzi theory applies to mixed variational problems under the form

$$\begin{cases} a(u,v) + b(p,v) = \langle f, v\rangle & \forall\ v \in V, \\ b(q,u) = \langle g, q\rangle & \forall\ q \in Q, \end{cases} \tag{58}$$

where $a(\cdot,\cdot) : V \times V \to \mathbb{R}$ and $b(\cdot,\cdot) : Q \times V \to \mathbb{R}$ are continuous bilinear forms, i.e.

$$a(u,v) \le \gamma_a\|u\|_V\|v\|_V \quad \forall\ u,v \in V, \qquad b(q,v) \le \gamma_b\|q\|_Q\|v\|_V \quad \forall\ q \in Q, \forall\ v \in V,$$

and $f \in V^*$, $g \in Q^*$. Such a variational problem is well posed if and only if the following (Brezzi) inf-sup conditions hold:

$$\inf_{u\in V_0}\sup_{v\in V_0}\frac{a(u,v)}{\|u\|_V\|v\|_V} = \inf_{v\in V_0}\sup_{u\in V_0}\frac{a(u,v)}{\|u\|_V\|v\|_V} = \alpha > 0, \tag{59}$$

[6] Throughout this section we use a notation which is as simple as possible and independent of the other sections for the sake of simplicity. We indicate as $V*$ the space of continuous and linar functionals on V, $\langle\cdot,\cdot\rangle$ the usual duality pairing between V and V^* and consider $f \in V^*$.

where $V_0 = \{v \in V : b(q,v) = 0,\ \forall q \in Q\}$, and

$$\inf_{q\in Q}\sup_{v\in V}\frac{b(q,v)}{\|q\|_Q\|v\|_V} = \beta_{BR} > 0. \tag{60}$$

Furthermore, under conditions (59)-(60) the unique solution $(u,p) \in V \times Q$ satisfies

$$\|(u,p)\|_{V\times Q} \le \mathcal{K}_{BR}(\alpha^{-1}, \beta_{BR}^{-1}, \gamma_a)\|(f,g)\|_{V^*\times Q^*}. \tag{61}$$

Moreover, it is also possible to derive the following estimates for the two variables distinctly:

$$\begin{aligned} \|u\|_X &\le \frac{1}{\alpha}\left[\|f\|_{X^*} + \frac{\alpha+\gamma_a}{\beta_{BR}}\|g\|_{Q^*}\right], \\ \|p\|_Q &\le \frac{1}{\beta_{BR}}\left[\left(1+\frac{\gamma_a}{\alpha}\right)\|f\|_{X^*} + \frac{\gamma_a(\alpha+\gamma_a)}{\alpha+\beta_{BR}}\|g\|_{Q^*}\right]. \end{aligned} \tag{62}$$

The relationship between the Brezzi theory and the Babuška theory in the case of a Stokes problem is based on the identifications (36)-(37): in this way, we can recast the mixed variational problem (58) into the Babuška framework; the error estimation (42) derived in Sec. 6 is the Babuška estimate (57) for (41). In the same way, using the estimations (62) on (40) it is possible to derive analogous error estimates for the velocity and the pressure errors, separately. The development of separated error bounds is ongoing. Moreover, it is possible to show that the main constants derived from these two theories are related[7] by [50]

$$\beta_{BA} \ge \frac{1}{\mathcal{K}_{BR}(\alpha^{-1}, \beta_{BR}^{-1}, \gamma_a)} \tag{63}$$

Thus, considering aggregate error estimates for both RB velocity and pressure of type (57) or (61), we have that the Babuška-based estimate is sharper than the Brezzi-based one since the "safety factor" β_{BA} is in any case greater than $1/\mathcal{K}_{BR}$. Moreover, the advantage of the Babuška-based error estimator is that only a (lower bound of a) stability constant needs to be evaluated to get the error bound. Instead, the Brezzi-based error estimator would require the evaluation of the coercivity/continuity constants of $a(\cdot,\cdot)$ and the Brezzi inf-sup constant of $b(\cdot,\cdot)$. We remark that all the approximation stability for the Stokes RB problem is based on Brezzi theory.

Appendix B: Offline-Online procedure for error bounds construction

In order to be computed in a very rapid and efficient way, the error estimation (42) has to be based on the Offline/Online procedure already used for the RB approximation. To reach this goal, it is important to introduce the Riesz representation of $r_{\mathbf{u}}(\cdot\,;\boldsymbol{\mu})$ and $r_p(\cdot\,;\boldsymbol{\mu})$: $\hat{\mathbf{e}}_{\mathbf{u}}(\boldsymbol{\mu}) \in X^{\mathcal{N}}$ and $\hat{e}_p(\boldsymbol{\mu}) \in Q^{\mathcal{N}}$ satisfy

$$(\hat{\mathbf{e}}_{\mathbf{u}}(\boldsymbol{\mu}), \mathbf{w})_X = r_{\mathbf{u}}(\mathbf{w};\boldsymbol{\mu}), \quad \forall \mathbf{w} \in X^{\mathcal{N}}, \quad (\hat{e}_p(\boldsymbol{\mu}), q)_Q = r_p(q;\boldsymbol{\mu}), \quad \forall q \in Q^{\mathcal{N}}. \tag{64}$$

[7] Following [8], it is also possible to show that $\beta_{BR} \ge \beta_{BA}$ and $\alpha \ge \beta_{BA}$.

This allows us to write (40) as

$$\begin{aligned} \mathcal{A}(\mathbf{e_u}(\boldsymbol{\mu}), \mathbf{w}; \boldsymbol{\mu}) + \mathcal{B}(e_p(\boldsymbol{\mu}), \mathbf{w}; \boldsymbol{\mu}) &= (\hat{\mathbf{e}}_\mathbf{u}(\boldsymbol{\mu}), \mathbf{w})_X \qquad \forall\ \mathbf{w} \in X^{\mathcal{N}}, \\ \mathcal{B}(q, \mathbf{e_u}(\boldsymbol{\mu}); \boldsymbol{\mu}) &= (\hat{e}_p(\boldsymbol{\mu}), q)_Q \qquad \forall\ q \in Q^{\mathcal{N}} \end{aligned}$$

and it follows that the dual norm of the residual can be evaluated through the Riesz representation:

$$\|r_\mathbf{u}(\cdot\,; \boldsymbol{\mu})\|_{X'} = \sup_{\mathbf{w} \in X^{\mathcal{N}}} \frac{r_\mathbf{u}(\mathbf{w}; \boldsymbol{\mu})}{\|\mathbf{w}\|_X} = \|\hat{\mathbf{e}}_\mathbf{u}(\boldsymbol{\mu})\|_X, \tag{65}$$

$$\|r_p(\cdot\,; \boldsymbol{\mu})\|_{Q'} = \sup_{q \in Q^{\mathcal{N}}} \frac{r_p(q; \boldsymbol{\mu})}{\|q\|_Q} = \|\hat{e}_p(\boldsymbol{\mu})\|_Q. \tag{66}$$

Hence, the error bounds developed in the previous section are only useful if they allow for an efficient Offline/Online computational procedure that leads to an Online complexity independent of $\mathcal{N}$. The Offline/Online decomposition presented in the following is mainly based on the dual norm of the residual. First of all, from the affine decomposition of bilinear forms (12) we can write, equivalently,

$$\tilde{\mathcal{A}}(\mathbf{V}, \mathbf{W}; \boldsymbol{\mu}) = \sum_{q=1}^{Q_a + 2Q_b} \tilde{\Theta}_q(\boldsymbol{\mu}) \tilde{\mathcal{A}}^q(\mathbf{V}, \mathbf{W}), \tag{67}$$

where

$$\begin{aligned} \tilde{\Theta}^q(\boldsymbol{\mu}) &= \Theta_a^q, && q = 1, \dots, Q_a, \\ \tilde{\Theta}^{q+Q_a}(\boldsymbol{\mu}) = \tilde{\Theta}^{q+Q_a+Q_b}(\boldsymbol{\mu}) &= \Theta_b^q(\boldsymbol{\mu}), && q = 1, \dots, Q_b, \end{aligned}$$

and

$$\begin{aligned} &\tilde{\mathcal{A}}^q(\mathbf{V}, \mathbf{W}) = \mathcal{A}^q(\mathbf{v}, \mathbf{w}) && q = 1, \dots, Q_a, \\ &\tilde{\mathcal{A}}^q(\mathbf{V}, \mathbf{W}) = \mathcal{B}^q(p, \mathbf{w}) && q = Q_a + 1, \dots, Q_a + Q_b, \\ &\tilde{\mathcal{A}}^q(\mathbf{V}, \mathbf{W}) = \mathcal{B}^q(q, \mathbf{v}) && q = Q_a + Q_b + 1, \dots, Q_a + 2Q_b. \end{aligned}$$

In this way, denoting as $\mathbf{U}_N(\boldsymbol{\mu}) = (\mathbf{u}_N(\boldsymbol{\mu}), p_N(\boldsymbol{\mu})) \in \mathbb{R}^{3N}$ the global vector of the RB components and recalling the expansion already used in (34), the residual can be expressed, considering the "global supremizer" option of Sec. 4.2, as

$$\tilde{r}(\mathbf{W}; \boldsymbol{\mu}) = \tilde{F}(\mathbf{W}) - \tilde{\mathcal{A}}(\mathbf{U}_N^{\mathcal{N}}(\boldsymbol{\mu}), \mathbf{W}; \boldsymbol{\mu}) = \tilde{F}(\mathbf{W}) - \sum_{n=1}^{3N} U_{N\,n}(\boldsymbol{\mu}) \sum_{q=1}^{\tilde{Q}} \tilde{\Theta}^q(\boldsymbol{\mu}) \tilde{A}^q(\boldsymbol{\Phi}_n, \mathbf{W}),$$

where $\tilde{Q} = Q_a + 2Q_b$ and $\boldsymbol{\Phi}_n = (\boldsymbol{\sigma}_n, 0)$ for $n = 1, \dots, 2N$, $\boldsymbol{\Phi}_n = (\mathbf{0}, \xi_n)$ for $n = 2N + 1, \dots, 3N$. Together with (64) and linear superposition, this gives us

$$\begin{aligned} (\hat{\mathbf{e}}(\boldsymbol{\mu}), \mathbf{W})_Y = (\hat{\mathbf{e}}_\mathbf{u}(\boldsymbol{\mu}), \mathbf{w})_X + (\hat{e}_p(\boldsymbol{\mu}), q)_Q = \\ \tilde{F}(\mathbf{W}) - \sum_{n=1}^{3N} U_{N\,n}(\boldsymbol{\mu}) \sum_{q=1}^{\tilde{Q}} \tilde{\Theta}^q(\boldsymbol{\mu}) \tilde{A}^q(\boldsymbol{\Phi}_n, \mathbf{W}) \end{aligned}$$

where $\hat{\mathbf{e}}(\boldsymbol{\mu}) = (\hat{\mathbf{e}}_\mathbf{u}(\boldsymbol{\mu}), \hat{e}_p(\boldsymbol{\mu})) \in Y^{\mathcal{N}}$. We thus may write $\hat{\mathbf{e}}(\boldsymbol{\mu}) \in Y^{\mathcal{N}}$ as

$$\hat{\mathbf{e}}(\boldsymbol{\mu}) = \tilde{\mathcal{F}} + \sum_{q=1}^{\tilde{Q}} \sum_{n=1}^{3N} \tilde{\Theta}^q(\boldsymbol{\mu}) U_{N\,n}(\boldsymbol{\mu}) \tilde{\mathcal{A}}_n^q,$$

where $\tilde{\mathcal{F}} \in Y^{\mathcal{N}}$ and $\tilde{\mathcal{A}}_n^q \in Y^{\mathcal{N}}$ (called FE "pseudo"-solutions) satisfy

$$(\tilde{\mathcal{F}}, \mathbf{W})_Y = \tilde{F}(\mathbf{W}), \quad \forall\ \mathbf{W} \in Y^{\mathcal{N}}, \tag{68}$$

$$(\tilde{\mathcal{A}}_n^q, \mathbf{W})_Y = -\tilde{A}^q(\boldsymbol{\Phi}_n, \mathbf{W}), \quad \forall\ \mathbf{W} \in Y^{\mathcal{N}},\ 1 \le n \le 3N,\ 1 \le q \le \tilde{Q}. \tag{69}$$

We note that (68) and (69) are simple parameter-independent problems and thus can be solved once in the Offline stage. It then follows that:

$$\|\hat{\mathrm{e}}(\boldsymbol{\mu})\|_Y^2 = \left(\tilde{\mathcal{F}} + \sum_{q=1}^{\tilde{Q}} \sum_{n=1}^{3N} \tilde{\Theta}^q(\boldsymbol{\mu}) U_{Nn}(\boldsymbol{\mu}) \tilde{\mathcal{A}}_n^q,\ \tilde{\mathcal{F}} + \sum_{q'=1}^{\tilde{Q}} \sum_{n'=1}^{3N} \tilde{\Theta}^{q'}(\boldsymbol{\mu}) U_{Nn'}(\boldsymbol{\mu}) \tilde{\mathcal{A}}_{n'}^{q'} \right)_Y =$$

$$(\mathcal{F}, \mathcal{F})_Y + \sum_{q=1}^{\tilde{Q}} \sum_{n=1}^{3N} \tilde{\Theta}^q(\boldsymbol{\mu}) U_{Nn}(\boldsymbol{\mu}) \left\{ 2(\tilde{\mathcal{F}}, \tilde{\mathcal{A}}_n^q)_Y + \sum_{q'=1}^{Q_a} \sum_{n'=1}^{N} \tilde{\Theta}^{q'}(\boldsymbol{\mu}) U_{Nn'}(\boldsymbol{\mu}) (\tilde{\mathcal{A}}_n^q, \tilde{\mathcal{A}}_{n'}^{q'})_Y \right\}. \tag{70}$$

This expression can be related to the requested dual norm of the residual through (65)-(66). It is the sum of products of parameter-dependent known functions and parameter independent inner products, formed of more complicated but precomputable quantities. The Offline/Online decomposition is thus clear:

(i) in the Offline stage we first solve (68), (69) for the parameter-independent FE "pseudo"-solutions $\tilde{\mathcal{F}}$ and $\tilde{\mathcal{A}}_n^q$, $1 \le n \le 3N$, $1 \le q \le \tilde{Q}$ and form/store the parameter-independent inner products $(\tilde{\mathcal{F}}, \tilde{\mathcal{F}})_Y$, $(\tilde{\mathcal{F}}, \tilde{\mathcal{A}}_n^q)_Y$ and $(\tilde{\mathcal{A}}_n^q, \tilde{\mathcal{A}}_{n'}^{q'})_Y$, $1 \le n, n' \le 3N$, $1 \le q, q' \le \tilde{Q}$. The Offline operation count depends on N, $\tilde{Q}$ and $\mathcal{N}$;

(ii) in the Online stage - performed for each new value of $\boldsymbol{\mu}$ - we simply evaluate the sum (70) in terms of the $\tilde{\Theta}^q(\boldsymbol{\mu})$, $1 \le q \le \tilde{Q}$ and $U_{N\,n}(\boldsymbol{\mu})$, $1 \le n \le 3N$ (already computed for the output evaluation) and the precomputed and stored (parameter-independent) $(\cdot,\cdot)_Y$ inner products. The Online operation count, and hence the marginal and asymptotic average cost, is only $\mathcal{O}(\tilde{Q}^2 9N^2)$, and thus the crucial point - the independence of $\mathcal{N}$ - is achieved again.

References

1. Babuška, I.: Error-bounds for finite element method. Numer. Math. **16**, 322–333 (1971)
2. Brezzi, F.: On the existence, uniqueness, and approximation of saddle point problems arising from Lagrangian multipliers. R.A.I.R.O., Anal. Numér. **2**, 129–151 (1974)
3. Brezzi, F., Fortin, M.: Mixed and Hybrid Finite Element Methods, *Springer Series in Computational Mathematics*, vol. 15. Springer Verlag (1991)
4. Brezzi, F., Rappaz, J., Raviart, P.: Finite dimensional approximation of nonlinear problems. Part I: Branches of nonsingular solutions. Numer. Math. **36**, 1–25 (1980)
5. Caloz, G., Rappaz, J.: Numerical analysis for nonlinear and bifurcation problems. In: P. Ciarlet, J. Lions (eds.) Handbook of Numerical Analysis, Vol. V, Techniques of Scientific Computing (Part 2), pp. 487–637. Elsevier Science B.V. (1997)
6. Dedè, L.: Optimal flow control for Navier-Stokes equations: Drag minimization. Int. J. Numer. Meth. Fluids **55**(4), 347–366 (2007)
7. Dedè, L.: Adaptive and reduced basis methods for optimal control problems in environmental applications. Ph.D. thesis, Politecnico di Milano (2008)
8. Demkowicz, L.: Babuška = Brezzi? Tech. Rep. 08-06, ICE, Univ. of Texas, Austin (2006)
9. Deparis, S.: Reduced basis error bound computation of parameter-dependent Navier-Stokes equations by the natural norm approach. SIAM J. Numer. Anal. **46**(4), 2039–2067 (2008)

10. Deparis, S., Løvgren, A.: Stabilized reduced basis approximation of incompressible three-dimensional Navier-Stokes equations in parametrized deformed domains. J. Sci. Comput. **50**, 198–212 (2012)
11. Deparis, S., Rozza, G.: Reduced basis method for multi-parameter-dependent steady Navier-Stokes equations: Applications to natural convection in a cavity. J. Comput. Phys. **228**(12), 4359–4378 (2009)
12. Gerner, A.L., Veroy, K.: Reduced basis a posteriori error bounds for the stokes equations in parametrized domains: a penalty approach. Math. Models Meth. Appl. Sci. **21(10)**, 2103–2134 (2010)
13. Gresho, P., Sani, R.: Incompressible Flow and the Finite Element Method: Advection-Diffusion and Isothermal Laminar Flow. John Wiley & Sons (1998)
14. Gunzburger, M.D.: Finite Element Methods for Viscous Incompressible Flows. Academic Press (1989)
15. Haasdonk, B., Salomon, J., Wohlmuth, B.: A reduced basis method for parametrized variational inequalities. Tech. Rep. 2011-16, SimTech preprint (2011)
16. Huynh, D., Knezevic, D., Chen, Y., Hesthaven, J., Patera, A.: A natural-norm successive constraint method for inf-sup lower bounds. Comput. Methods Appl. Mech. Engrg. **199**(29-32), 1963 – 1975 (2010)
17. Huynh, D., Rozza, G., Sen, S., Patera, A.: A successive constraint linear optimization method for lower bounds of parametric coercivity and inf-sup stability costants. C. R. Acad. Sci. Paris. Sér. I Math. **345**, 473–478 (2007)
18. Ito, K., Ravindran, S.: A reduced-order method for simulation and control of fluid flow. J. Comput. Phys. **143**(2), 403–425 (1998)
19. Knezevic, D., Nguyen, N., Patera, A.: Reduced basis approximation and a posteriori error estimation for the parametrized unsteady Boussinesq equations. Math. Models Meth. Appl. Sci. **21(7)**, 1415–1442 (2011)
20. Lassila, T., Rozza, G.: Parametric free-form shape design with PDE models and reduced basis method. Comput. Methods Appl. Mech. Engrg. **199**, 1583–1592 (2010)
21. rbMIT Library: `http://augustine.mit.edu/methodology/methodology_rbMIT_System.htm`. MIT, Cambridge (2007–2010). ©Massachusetts Institute of Technology
22. Løvgren, A., Maday, Y., Rønquist, E.: A reduced basis element method for the steady Stokes problem. ESAIM Math. Modelling Numer. Anal. **40(3)**, 529–552 (2006)
23. Manzoni, A., Quarteroni, A., Rozza, G.: Shape optimization of cardiovascular geometries by reduced basis methods and free-form deformation techniques. Int. J. Numer. Meth. Fluids **70**(5), 646–670 (2012)
24. Manzoni, A., Rozza, G.: A posteriori error estimation for quadratic outputs in parametrized stokes problems. in preparation (2012)
25. Milani, R., Quarteroni, A., Rozza, G.: Reduced basis method for linear elasticity problems with many parameters. Comput. Methods Appl. Mech. Engrg. **197**, 4812–4829 (2008)
26. Nguyen, N., Veroy, K., Patera, A.: Certified real-time solution of parametrized partial differential equations. In: Handbook of Materials Modeling, (S. Yip, editor), Springer, pp. 1523–1558 (2005)
27. Noor, A.: On making large nonlinear problems small. Comput. Methods Appl. Mech. Engrg. **34:955-985** (1982)
28. Noor, A., Peters, J.: Reduced basis technique for nonlinear analysis of structures. AIAA Journal **18(4):455-462** (1980)
29. Panton, R.L.: Incompressible Flow, 3rd edn. John Wiley & Sons, Inc. (2005)
30. Patera, A., Rozza, G.: Reduced Basis Approximation and A Posteriori Error Estimation for Parametrized Partial Differential Equations. Version 1.0, 2006, Copyright MIT, to appear in (tentative rubric) MIT Pappalardo Graduate Monographs in Mechanical Engineering. Available at `http://augustine.mit.edu`
31. Peterson, J.: The reduced basis method for incompressible viscous flow calculations. SIAM J. Sci. Stat. Comput. **10(4):777-786** (1989)
32. Pierce, N., Giles, M.: Adjoint recovery of superconvergent functionals from pde approximations. SIAM Rev. **42**(2), 247–264 (2000)
33. Quarteroni, A.: Numerical Models for Differential Problems. Springer, Series MS&A , Vol. 2 (2009)
34. Quarteroni, A., Rozza, G.: Numerical solution of parametrized Navier-Stokes equations by reduced basis methods. Numer. Methods Partial Differential Equations **23**(4), 923–948 (2007)

35. Quarteroni, A., Valli, A.: Numerical Approximation of Partial Differential Equations. Springer-Verlag (1994)
36. Rovas, D.: Reduced-basis output bound methods for parametrized partial differential equations. Ph.D. thesis, Massachusetts Institute of Technology (2003)
37. Rozza, G.: On optimization, control and shape design of an arterial bypass. Int. J. Numer. Meth. Fluids **47**(10–11), 1411–1419 (2005)
38. Rozza, G.: Real-time reduced basis techniques for arterial bypass geometries. In: K. Bathe (ed.) Computational Fluid and Solid Mechanics, pp. 1283–1287. Elsevier (2005). Proceedings of the Third M.I.T. Conference on Computational Fluid and Solid Mechanics, June 14-17, 2005
39. Rozza, G.: Shape design by optimal flow control and reduced basis techniques: applications to bypass configurations in haemodynamics. Ph.D. thesis, N. 3400, École Polytechnique Fédérale de Lausanne (2005)
40. Rozza, G.: Real-time reduced basis solutions for Navier-Stokes equations: optimization of parametrized bypass configurations. In: Proceedings of the ECCOMAS CFD 2006, IV European Conference on Computational Fluid Dynamics, Egmond aan Zee, The Netherlands, P. Wesseling, E. Onate, J. Periaux (Eds) (2006)
41. Rozza, G.: Reduced basis methods for Stokes equations in domains with non-affine parameter dependence. Comput. Vis. Sci. **12(1)**, 23–35 (2009)
42. Rozza, G.: Reduced basis approximation and error bounds for potential flows in parametrized geometries. Commun. Comput. Phys. **9**, 1–48 (2011)
43. Rozza, G., Huynh, D., Patera, A.: Reduced basis approximation and a posteriori error estimation for affinely parametrized elliptic coercive partial differential equations. Arch. Comput. Methods Engrg. **15**, 229–275 (2008)
44. Rozza, G., Lassila, T., Manzoni, A.: Reduced basis approximation for shape optimization in thermal flows with a parametrized polynomial geometric map. In: Spectral and High Order Methods for Partial Differential Equations. Selected papers from the ICOSAHOM '09 conference, June 22-26, Trondheim, Norway. Springer, Series: Lecture Notes in Computational Science and Engineering, vol. 76, J.S. Hesthaven, E.M. Rønquist (Eds.) (2011)
45. Rozza, G., Manzoni, A.: Model order reduction by geometrical parametrization for shape optimization in computational fluid dynamics. In: Proceedings of ECCOMAS CFD 2010, V European Conference on Computational Fluid Dynamics, Lisbon, Portugal, J.C.F. Pereira and A. Sequeira (Eds) (2010)
46. Rozza, G., Nguyen, C., Patera, A., Deparis, S.: Reduced basis methods and a posteriori error estimators for heat transfer problems. In: Proceedings of HT2009, 2009 ASME Summer Heat Transfer Conference, paper HT 2009–88211 (2009)
47. Rozza, G., Veroy, K.: On the stability of the reduced basis method for Stokes equations in parametrized domains. Comput. Methods Appl. Mech. Engrg. **196**(7), 1244–1260 (2007)
48. Veroy, K., Patera, A.: Certified real-time solution of the parametrized steady incompressible Navier-Stokes equations: rigorous reduced-basis a posteriori error bounds. Int. J. Numer. Meth. Fluids **47**, 773–788 (2005)
49. Veroy, K., Prud'homme, C., Rovas, D.V., Patera, A.T.: *A Posteriori* error bounds for reduced-basis approximation of parametrized noncoercive and nonlinear elliptic partial differential equations. In: Proceedings of the 16th AIAA Computational Fluid Dynamics Conference (2003). Paper 2003-3847
50. Xu, J., Zikatanov, L.: Some observation on Babuška and Brezzi theories. Numer. Math. **94**(1), 195–202 (2003)